Internship Report

Review of the impact of hydrogen addition to natural gas on gas turbine combustion

Marc Bus
S0178934
06-06-2013

Placement report

Review of the impact of hydrogen addition to natural gas on gas turbine combustion

Marc Bus
S0178934

E.ON New Build and Technology
Gas Turbine Combustion department
Ratcliffe-on-Soar, Nottingham, UK

Supervisor:
Dave Abbott

Line manager:
Cath Goy

University of Twente
Thermal Engineering group
Enschede, the Netherlands

Supervisor:
Jim Kok

Period:
October 1-2012 to March 31-2013

Summary

I In the future there will be a greater need to store energy as there will be more renewable energy which has a fluctuating output. One way of storing this energy is by producing hydrogen out of it and storing it in the gas grid, providing all users with a hydrogen enriched gas. This report will look at the effects of this hydrogen enrichment up to 20%vol on the combustion in gas turbines.

II The current UK regulations do not allow hydrogen in the national gas grid. If hydrogen is to be injected into the gas grid for storage, new regulations will have to be made. The gas turbine manufacturers use less stringent limits for hydrogen; however the maximum amount differs per manufacturer. At the moment typically up to about 5%vol hydrogen is allowed in a gaseous fuel for a modern lean premixed combustion system. Some gas do allow higher levels, but this is rare for large utility power generation systems.

III In the past various models have been developed to predict the interchangeability of different gases; three of these models have been used in the current work to investigate the impact of hydrogen addition on natural gas. The models used are the AGA Bulletin 36, Weaver and Dutton models. They all use indices based on flame behaviour to create a region of interchangeability. These methods were developed for use on domestic appliances and the limits are set based on experimental data.

IV The literature review is split into four main categories: flame speeds, emissions, combustion dynamics and flashback. There are a number of relations that describe the laminar flame speed; the Bougrine relation appears to be the best one, however its limitations must be kept in mind when using it. The turbulent flame speed can be reasonably described with one of the Lipatnikov and Chomiak or Brower correlations. To calculate the turbulent flame speed some turbulent flame properties have to be known; as these are difficult to determine the turbulent flame speed will be hard to capture. The emissions of CO and NO_x are the most important. Due to their opposite temperature dependence they create an operating window in which the temperature is limited by the level of emissions. The combustion dynamics can be investigated by looking at the turbulent source term, with the laminar flame speed as one of its parameters, and the flame transfer function, which depends on the expansion ratio and burning time. For flashback four different mechanisms are identified; the two most important are combustion induced vortex breakdown (CIVB) and wall boundary layer flashback (WBLF).

V After the literature study the most promising methods found were reviewed for their suitability to get a better understanding of the effects of hydrogen addition. CHEMKIN PREMIX was used to simulate a freely propagating flame. This method gives information about the laminar flame speed, flow properties and species mole fractions. The sensitivity of the three turbulent flame speed correlations was investigated, focussing on the uncertainty in the velocity fluctuations, turbulent length scale and laminar flame speed. The Characteristic combustion time calculations give an indication about the time needed for the temperature to rise from its minimum to maximum or from 10% to 90% of the temperature change. The expansion ratio is calculated based on a basic approach to combustion. The Konle and Gradient models were reviewed for assessing the likelihood of CIVB and WBLF flashback respectively.

VI After describing the methods used, their results have been shown. For CHEMKIN an indicative validation of the GRI 3.0 reaction scheme was shown next to the results of the species profiles, which included the emissions, laminar flame speeds and the burning time. The expansion ratio was calculated and the results presented in two ways. Finally the CHEMKIN laminar flame speeds were used to predict the likelihood of flashback with the Konle model.

VII After performing the calculations the results were thoroughly analysed. The effect of hydrogen on the laminar flame speed was up to 10% at 20%vol hydrogen, which was less than expected. The turbulent flame speed predictions were not unambiguous, because the results strongly depended on the chosen correlation. Based on the Brower correlation there was an increase of about 22% at 20%vol hydrogen. The emissions did not change very much when hydrogen was added, the NO_x remained the same and the CO may decreased slightly. The combustion dynamics would be unlikely to show major changes as the flame transfer function and the impact on the laminar flame speed depending turbulent source term do not change much. Based on the Konle model, only a minor increase in flashback risk was predicted when hydrogen was added, due to its dependence on the laminar flame speed.

VIII The methods used indicate that low levels of hydrogen are unlikely to cause problems, but it is not possible to define a maximum limit based on this report. The analysis of the results indicates that only the increase turbulent flame speed may cause some problems as it increases by about 22% at 20%vol hydrogen addition; this prediction strongly depends on the correlation and estimations used.

Since not all the calculations could be compared with results from literature, some level of uncertainty is still present in the results. It is recommended that new developments with regards to hydrogen addition to natural gas are followed. Further it would be recommended to perform experiments at conditions that are more relevant to gas turbine conditions, as this will give a good indication of the impact of hydrogen. The conditions used for the calculations are very similar to base load gas turbine conditions, it is likely that during start up the conditions differ, so the impact of hydrogen on the start up should also be reviewed.

Contents

Summary **3**

Contents **5**

Nomenclature **7**

Abbreviations 7

Symbols 7

1 Introduction **8**

2 Current regulations **9**

2.1 Gas specifications 9

2.2 Manufacturer gas specifications 10

3 Interchangeability methods **13**

3.1 Wobbe index 13

3.2 AGA #36 indices 14

3.3 Weaver Indices 15

3.4 Dutton diagram 17

3.5 Multiple index interchangeability method limitations 18

4 Literature review **19**

4.1 Laminar flame speed 19

4.2 Turbulent Flame speed 24

4.3 Emissions 28

4.4 Combustion Dynamics 31

4.5 Flashback 33

5 Review of assessment tools/methods **34**

5.1 CHEMKIN 34

5.2 Turbulent flame speed correlation sensitivity 37

5.3 Volumetric expansion ratio 42

5.4 Konle model for CIVB 42

5.5 Gradient method for WBLF 43

6 Analysis at gas turbine conditions 44
6.1 PREMIX results 44
6.2 Turbulent flame speed 53
6.3 Expansion ratio calculations 55
6.4 Konle model results 55

7 Discussion of results 57
7.1 Flame speeds 57
7.2 Emissions 57
7.3 Combustion Dynamics 58
7.4 Flashback 58

8 Conclusions and recommendations 59
8.1 Conclusions 59
8.2 Recommendations 60

References 61

Appendix I Bougrine flame speed correlation 64
Appendix II Cardiff rig testing program 65
Appendix III Analysis of the complete GT load range 66

Nomenclature

Abbreviations

AGA	American Gas Association
ATM	Atmosphere
CIVB	Combustion Induced Vortex Breakdown flashback
DLR	Deutsches Zentrum für Luft- und Raumfahrt, German Aerospace Centre
EASEE	European Association for Streamlining of Energy Exchange
EPR	Expansion Ratio
EQR	Equivalence Ratio
GE	General Electric
GRI	Gas Research Institute
GS(M)R	Gas Safety (Management) Regulations
GT	Gas Turbine
ICF	Dutton’s Incomplete Combustion Factor
LI	Dutton’s Lifting Index
NASA	National Aeronautics and Space Administration
RD	Relative Density
SI	Dutton’s Soothing Index
WBLF	Wall boundary Layer Flashback
WN	Dutton’s Wobbe Number

Symbols

C_P	Specific Heat at constant pressure	J/kgK
D	Mass diffusion	m^2/s
d	Diameter	m
g_{crit}	Critical wall velocity gradient	1/s
HHV	Higher heating value	MJ/m^3 at 15°C, 15°C
LHV	Lower heating value	MJ/m^3 at 15°C, 15°C
M	mass flow	kg/s
P	Pressure	bar or atm
RD	Relative density	-
S_L	Laminar flame speed	m/s
S_T	turbulent flame speed	m/s
T	Temperature	°C or K
U	Mean flow velocity	m/s
V	Volume flow	m^3/s
WI	Wobbe Index	MJ/m^3 at 15°C
u’	Velocity Fluctuations	m/s
α	Thermal Diffusivity	m^2/s
λ	Thermal Conductivity	W/mK
μ	Dynamic Viscosity	Pa s (kg/ms)
ν	Kinematic Viscosity	m^2/s
ρ	Density	kg/m^3
ϕ	Equivalence ratio	-

1 Introduction

Due to the increasing use of renewable energy sources there is a risk that they will produce a surplus of energy on a very sunny or windy day. At the moment these units are turned down when the supply exceeds the demand, so the full potential of these units is not used. One of the current ideas is that this excess energy can be stored by electrolysing water to produce hydrogen. The hydrogen will be added to the gas transmission or distribution grid where it will be stored and transported. At the moment E.ON is building a pilot plant in Falkenhagen, Germany where this energy storage method will be demonstrated.

The consequence of adding hydrogen to the gas grid is that the natural gas in it will be enriched with hydrogen affecting all the gas users; these include E.ON's power stations. As the hydrogen addition causes a change in fuel quality all aspects of the combustion process will be affected just as any other change in fuel quality. At the moment there is not a lot known about the effects of hydrogen addition to natural gas on the combustion in gas turbines.

This report will serve as a first step in developing an understanding of the effects of adding hydrogen up to 20%vol to natural gas on the combustion in gas turbines. As all the aspects of the combustion process are affected this will be a very broad study. First the current regulations for hydrogen in the gas grid and gas turbines are reviewed. This is followed by a literature study on the effects of hydrogen addition. The literature study is divided into four main topics: (laminar and turbulent) flame speeds, emissions, combustion dynamics and flashback. The models found in the literature will be combined with calculations performed with CHEMKIN PREMIX to get a better understanding of the effects of hydrogen on the four topics. After a thorough analysis of the results, conclusions and recommendations are made on the effects of hydrogen addition.

2 Current regulations

The current regulations have been reviewed with respect to the addition of hydrogen to natural gas. Firstly, the regulations set by European governments for the national gas grids have been assessed, followed by the limitations set by the gas turbine manufacturers. As will be shown below, there is some variation in allowance between both sets of regulations/limitations.

2.1 Gas specifications

To make sure that (domestic) appliances perform to their design specifications there is a need to certify the quality of the gas they will encounter. The key requirement is that the consumer does not see any significant difference in performance of their device when it uses gas from different sources. The Gas Safety (Management) Regulations (GS(M)R) [1] provide the current specifications for the natural gas in the UK as shown in Table 1.

Due to the globalisation of the energy market and the decline in UK gas production there is an increase in natural gas imports. Each country has its own set of regulations based on their historic supply of gas [2]. This is indicated in Figure 1 below in which the allowed Wobbe Index range is shown for different countries [3] and the Wobbe Indices of the typical gas mixtures received there.

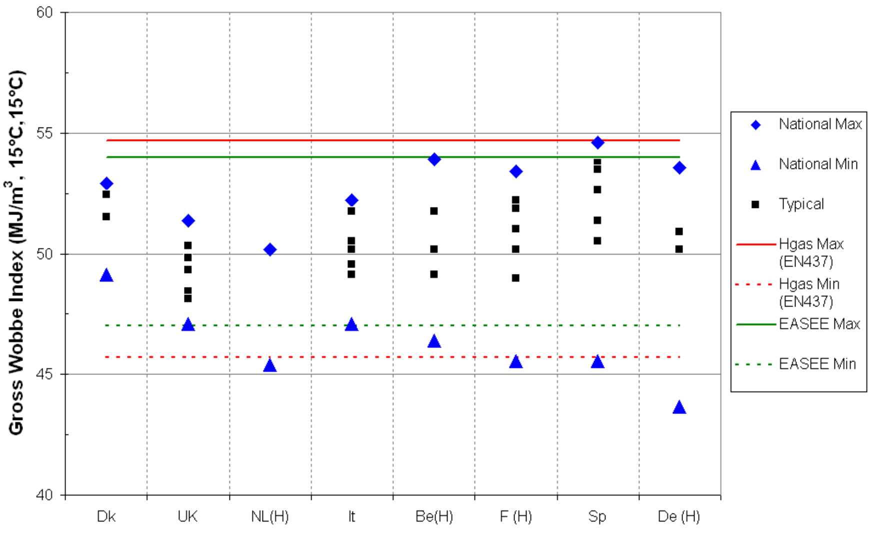

Figure 1 Indicative European Gas specifications

Parameter\Standard	UK GS(M)R	EASEE gas	Typical UK gas
Wobbe Index (MJ/Nm^3) 15°C	47.2 – 51.41	47.0 – 54.0	39 – 40
Hydrogen	Max 0.1 mol %	Insignificant	x
Incomplete combustion index (ICF)	Max 0.48	Not specified	x
Sooting index (SI)	Max 0.60	Not specified	x
Relative density (RD)	Not specified	0.5548 – 0.70	0.62 – 0.65

Table 1 Gas regulations

Currently the European Committee for Standardisation (CEN) is working on a European gas standard. Before the European Committee issued this study there was a standard developed by the European Association for Streamlining of Energy Exchange (EASEE) to simplify the transfer and trading of natural gas; this is known as the EASEE-gas standard [4]. This standard is shown in Table 1 and Figure 1. The ICF and SI indices are a way of determining the interchangeability and performance of a gas based on Dutton's method; this will be explained in more detail in Section 3.4.

The UK natural gas composition has historically been stable, but is showing more variation. This variation is likely to increase further in the future, but as long as the gas composition meets the regulations there should be not much difference noticeable for the consumer. However the industrial users, like power stations, may experience problems even when the natural gas fulfils the regulations, due to their more sensitive equipment.

The addition of hydrogen is currently effectively prohibited by the regulations in the UK, because these allow only a very small amount of hydrogen. If hydrogen is to be added to the UK gas grid then it will be necessary to change the current regulations, however this is not necessarily the case in other European countries.

2.2 Manufacturer gas specifications

Each gas turbine manufacturer has its own specifications for the fuel that can be used without problems in each of their gas turbines, but in general the operating ranges are similar. This may not be directly clear when the fuel specifications are compared; therefore a comparison is included between the different gas turbines with the same set of parameters.

2.2.1 Manufacturer specifications

Gas turbine fuel specifications are normally contractual documents relating to a particular contract and are confidential and cannot be referenced directly here. However the majority large power generation gas turbines with lean premixed combustion systems have fuel specifications that allow very low levels (0-1%vol) or moderate levels (~5%vol) of hydrogen to be present in natural gas; higher levels of hydrogen are unusual.

Gas turbine manufacturers typically specify [30] that their turbines are capable of operating over a wide range of Wobbe Index(WI), see also section 3.1, and Heating Value. Ranges in excess of ±10% of mid-range values are normal. However, it is unlikely that this could be accommodated without re-tuning of the gas turbine and some combustors may need minor hardware changes. For a particular gas turbine installation a range of ±5% of the tuned value of WI (and/or Heating Value) is typical. However for some gas turbines a range of only ±2% of the WI has been specified.

The detailed composition also affects combustion performance including flame stability, emissions, flashback and ignition properties. Manufacturers' specifications account for such compositional changes in different ways, but they typically specify maximum levels of higher hydrocarbons (ethane, propane, butane etc), minimum methane and/or maximum inerts. These specifications aim to ensure that the fuel gas is predominantly methane, and that gases which contain both high levels of inerts and higher hydrocarbons, but are still within WI limits, are not allowed [30].

2.2.2 Gas Turbine fuel range charts

As indicated in the previous section, different gas turbines have different descriptions of the acceptable fuel range. To make a comparison between the acceptable fuels for E.ON's main gas turbine types a Monte-Carlo type approach is used to determine the allowed fuel range. In the approach a thousand gas compositions are randomly generated within a certain set of rules, which are described below.

An initial amount of methane is determined, for which a lower limit is in place, and the rest of the mixture is made up out of higher hydrocarbons, where the amount of C_n is always larger than the amount of C_{n+1}. A random amount of nitrogen and carbon dioxide can be added up to a certain maximum limit. After the creation of the components of the mixture it is normalised, so that the sum of the mole fractions equals one.

The next step is determining the gas properties which are needed for testing against particular gas turbine requirements. The fuel requirements for the following E.ON gas turbines were evaluated:

- Enfield Power Station (GT 26B)
- Connah's Quay Power Station (GE 9FA)
- Cottam Development Centre (Siemens SGT5-4000F)

It was assumed that the gas turbines were tuned for Lupton gas, as this is a typical UK natural gas [5] and its composition is given in Table 2. The acceptability of each of the one thousand gasses were assessed for the acceptability of the sites and the results are shown in Figure 2, Figure 3 and Figure 4.

Component	CH_4	C_2H_6	C_3H_8	C_4H_{10}	C_5H_{12}	N_2	CO_2	Sum
[%(vol)]	87.21	6.18	1.74	0.19	0.54	1.69	2.45	100

Table 2 Composition of a typical UK natural gas (Lupton [5])

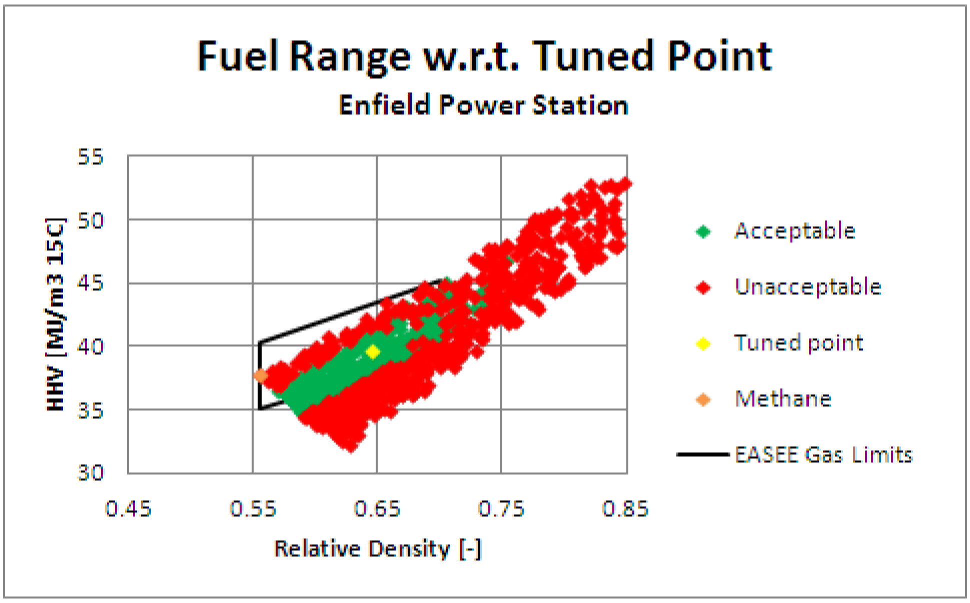

Figure 2 Enfield Power Station: Acceptable fuels when tuned a typical UK gas

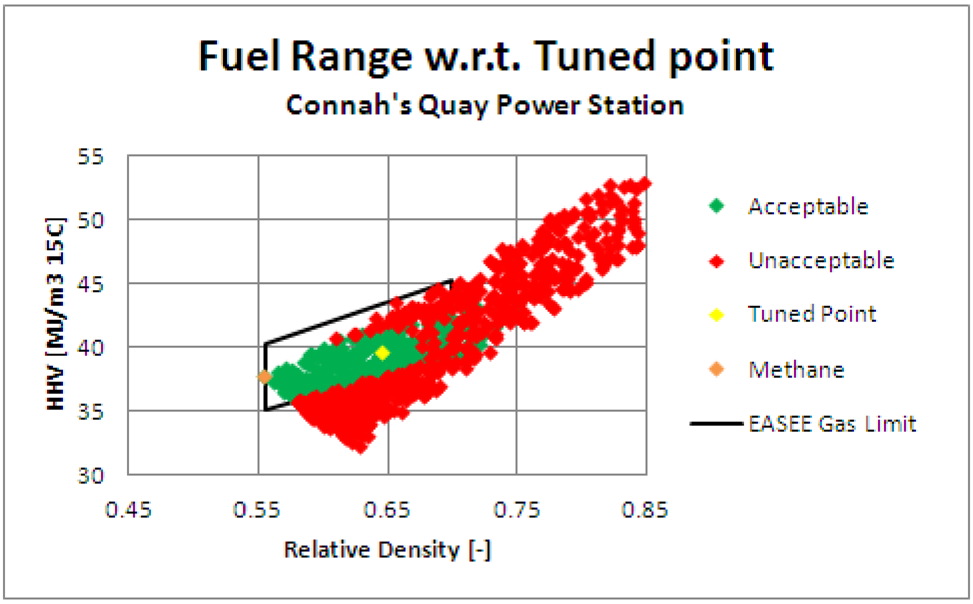

Figure 3 Connah's Quay Power Station: Acceptable fuels when tuned a typical UK gas

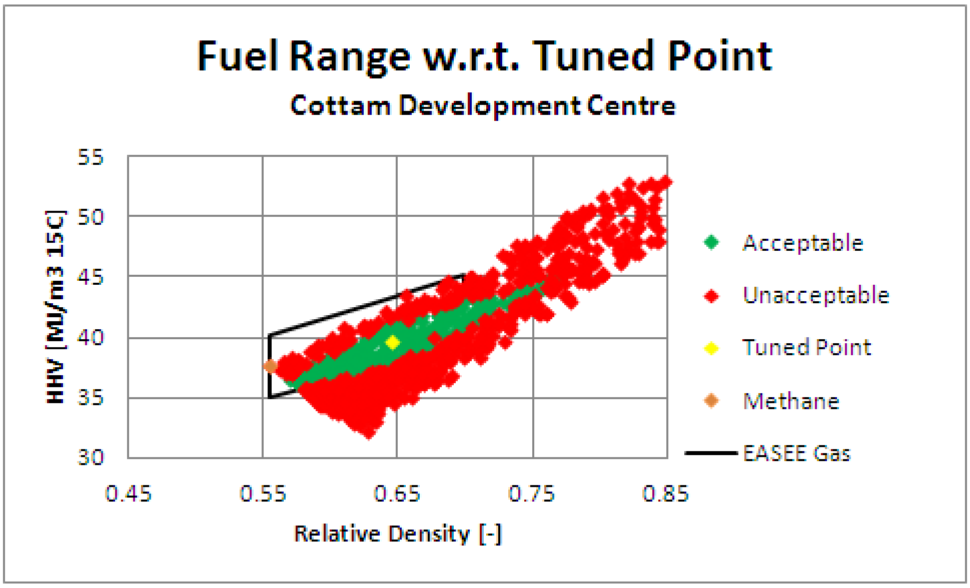

Figure 4 Cottam Development Centre Acceptable fuels when tuned a typical UK gas

These figures confirm that the gas turbines all have similar ranges of allowable gases; the differences are caused by the different ways in setting the specifications.

The disadvantage of this Monte-Carlo type approach is that some gases are generated which are unlikely to be found in nature, these gases appear in the figures as the red dots in the green area. Despite this minor disadvantage this method is useful to get a general understanding of the operating range of the different gas turbines.

3 Interchangeability methods

There are different methods of comparing the interchangeability of gases; roughly the methods can be split into single index and multiple index methods. The single index methods are based on properties of the gases, like the density or heating value, or a combination of these, like the Wobbe Index .The multiple index models are based on combustion phenomena, like flashback and yellow tipping. These indices are more complex, because often one has to know the gas composition.

The Single Index that is used the most is the Wobbe index. The Weaver indices and the AGA #36 indices are the most commonly used multiple index methods. A special group of multiple index models are the graphs that describe interchangeability. These graphs often use a few parameters to construct a region of interchangeability, an example of which is the Dutton diagram.

The method used to measure interchangeability varies per country. The AGA and Weaver indices are often used in the USA, the Dutton diagram is used in the UK, and countries in Europe tend to use a range of graphical methods or the Wobbe Index in combination with some additional limitations to determine the interchangeability of gases.

The limits for both models are determined by previous experience or testing appliances. When the appliances are tested the performance is measured with respect to the gas that the appliance was designed for, the so called adjustment gas. The gases that are used for testing are referred to as substitute gases, in the past these tests were important due to the regional variation in gas quality. These limits are empirical rather than fundamental. Sometimes there are different limitations for one index for different fuel types.

3.1 Wobbe index

The Wobbe Index is a measurement of the heat input into the combustor. It is normally defined as the ratio of the heating value, and the square root of the relative density, see equation (1). The specific density is a dimensionless density, the density of the gas is divided by the density of air, both measured at standard conditions. There are different methods of calculating the Wobbe Index, it can be based on the lower or higher heating value and it could be temperature dependent, making it important to verify how it is defined.

$$WI = \frac{HHV}{\sqrt{RD}} \quad \left[\frac{MJ}{m^3}\right] \tag{1}$$

In contrast to most of the numbers used in engineering, like the Reynolds or Mach number, the Wobbe Index is not dimensionless. When one gas is replaced by another gas with the same Wobbe Index, then the heat input is the same, so the fuel valve maintains the same position if the system is controlled to maintain combustion temperature.

Effects on the flame speed or chemical kinetics are not described by the Wobbe Index, so two gases having the same Wobbe Index might behave very differently. Therefore it is necessary to look at other indices too during the determination of the interchangeability of fuels.

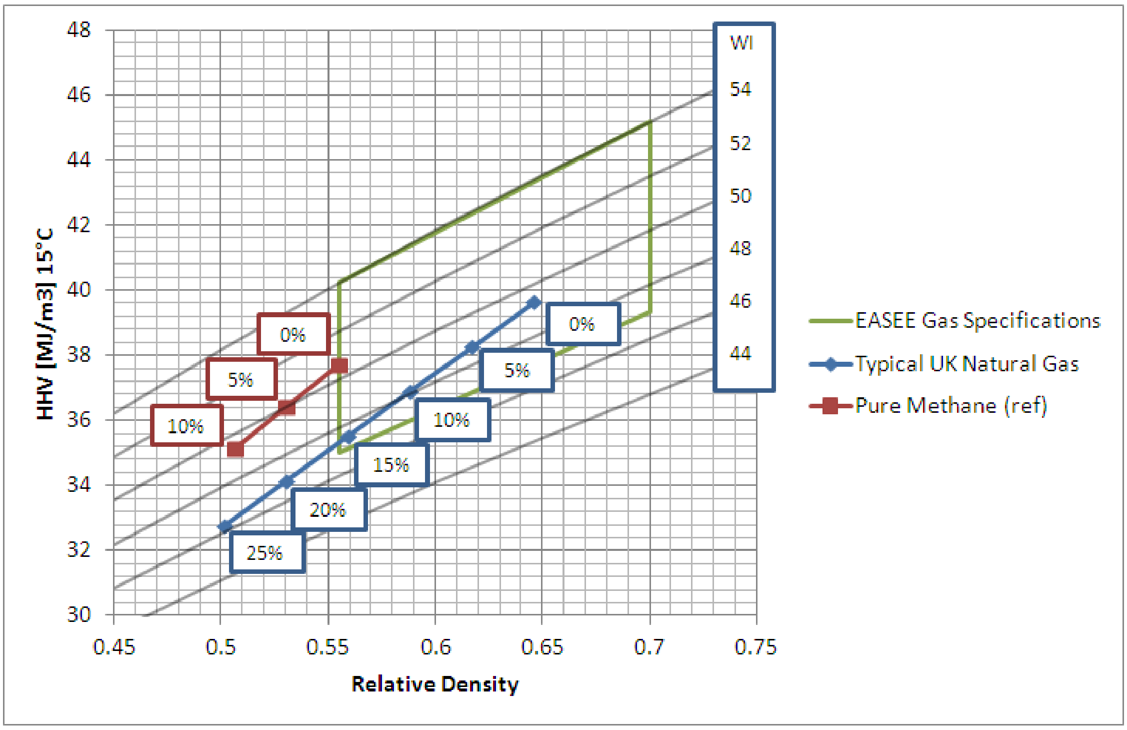

Figure 5 Effect of hydrogen addition on the Wobbe Index and relative density

To get a general idea of the effects of adding hydrogen it is interesting to look at the relative density, heating value and Wobbe Index. Hydrogen causes a decrease in the heating value and specific gravity. This is shown in Figure 5 for methane and a typical UK natural gas. The lines start with the hydrogen free gas and hydrogen is added in steps of 5%vol.

The EASEE-gas limits are also plotted in the figure. The top and bottom side of the box are lines with a constant Wobbe Index of respectively 54 and 47. Based on this figure, the addition of hydrogen up to 15%vol to a typical UK natural gas would still be acceptable according to the EASEE-gas specification for Wobbe Index and Relative Density.

3.2 AGA #36 indices

The AGA indices were published in 1946 by the American Gas Association Laboratories as Research Bulletin 36 [6, 43]. They looked at the interchangeability of natural gases by studying a wide variety of gases in (domestic) appliances. At this time it was becoming clear that a one index model could not describe interchangeability sufficiently, so they developed a model that contained three indices. They based their indices on important combustion properties; the properties they chose were: lifting, yellow tipping and flashback, their indices are noted by I_L, I_Y, I_F respectively.

Yellow tips indicate that soot is being formed in the flame. Lifting is the flame moving downstream with the flow away from the burner, and flashback occurs when the flame moves upstream into the burner.

3.2.1 AGA flashback index (I_F)

The flashback index is calculated with respect to the adjustment (original) gas. If this value exceeds the limit of 1.18, the general limit set by AGA, there is a significant risk of flashback [7]. The flashback index can be calculated with the expression (2). It compares the lifting limit constant (K_i), the lifting constant (F_i), the air factor (f_i), heating value (h_i) and the specific gravity of the adjustment and substitute gases (d_i). The index i indicates the use for the substitute (s) and adjustment (a) gas. The index j denotes the summation of all the species present in the gas.

$$I_F = K_s f_s \frac{\sqrt{\frac{h_s}{1000}}}{K_a f_a}, \tag{2}$$

$$with\ f_i = \frac{1000\sqrt{d_i}}{h_i}\ and\ K_i = \frac{F_i}{d_i}\ with\ F_i = \sum_j x_j F_j$$

The values of this index are plotted in Figure 6; the area below the limit line defines the area of interchangeability. However one can find different maximum values for the flashback factor in the literature, creating different levels of interchangeability. The limit that is shown here is the one that was proposed by the AGA researchers, other values can be found in literature [8], however they do not clearly state why the value is different.

3.3 Weaver Indices

Some researchers found that the AGA #36 indices did not match well with their experimental results and hoped that an improved formula could be developed. Weaver accepted this challenge and came up with his own set of formulas [6, 43]. He produced a set of four parameters that describe the main combustion parameters: the lifting (J_L), flashback (J_F), yellow tipping (J_Y) and soothing (J_I), which all depend on the Weaver flame speed factor (S).

3.3.1 Weaver flame speed factor (S)

The Weaver flame speed factor (S) describes the approximate maximum velocity with which a flame can travel in any gas-air mixture. There is no easy and accurate way to calculate the flame speed, therefore some assumptions have to be made. The principal assumption that is made is that the maximum flame velocity in mixtures of two fuel gases is a linear function of the volumes obtained by adding to each gas in the mixture the volume of air required for its complete combustion. So that S can be calculated with formula (3).

$$S = \frac{aF_a + bF_b + cF_c + \ldots}{A + 5Z - 18.8Q + 1}\ with\ F_a = \frac{(A+1)U_a}{U_{H_2}} * 100\% \tag{3}$$

	Relative Density (D_i)	Air requirement (A_i)	Flame speed factor (F_i)
CH_4	0.55	9.55	148
C_2H_6	1.04	16.71	301
C_3H_8	1.56	23.87	398
C_4H_{10}	2.09	31.03	513
H_2	0.07	2.39	339

Table 3 Properties of natural gas for the Weaver indices [6]

In the formula are a,b,c, etc the volume fractions of the combustible contents of the fuel gas, F_a, F_b, F_c, etc are the flame speed factors of the corresponding gas according to, A is the volume of air required to burn 1 volume of gas, Z is the fraction by volume of the inert gases and Q is the fraction of oxygen in the fuel. The factors $F_{(a,\ b,\ c\ldots)}$ are calculated by recording the maximum ignition velocity (U) of the combustible with air as a percentage of the maximum ignition value of hydrogen (U_{H2})

with air and then multiplied by one plus the number of cubic feet required to burn 1 cubic foot of gas, as shown in Table 3.

3.3.2 Weaver Flashback Index (J_F)

The coefficient J_F will describe the likelihood of flashback to occur. The index is based on comparing the ratio of the Weaver flame speed factors (S/S_a), and the air requirements $A\sqrt{D_a}/A_a\sqrt{D}$ (equals J_A) of the substitute and adjustment gas. When two gases are completely interchangeable with respect to flashback J_F equals zero.

J_F can be calculated with formula (4). The correlation depends on the Weaver flame speed (S), the amount of air needed for the complete combustion of the fuel (A) and the specific gravity of the gas (D), the subscript a denotes the adjustment gas and no subscript the substitute gas. The results of this formula are plotted in Figure 6 together with the AGA flashback index.

$$J_F = C - C_a = \frac{S}{S_a} - 1.4\,\frac{A\sqrt{D_a}}{A_a\sqrt{D}} + 0.4 \qquad (4)$$

In this report the high methane limit is chosen for the flashback limit, this limit has a value of 0.7 and when J_F exceeds this value flashback becomes a danger.

3.3.3 Comparing J_F with I_F

In Figure 6 the values of the flashback index are plotted versus the amount of hydrogen added to the original fuel, for methane and typical UK natural gas. Both methods show that up to about 25% of hydrogen can be added without risking flashback. It is interesting that there is a small difference in the likelihood of flashback between the two methods with respect to the original gas, because the gas that flashes back the first changes depending on the method used.

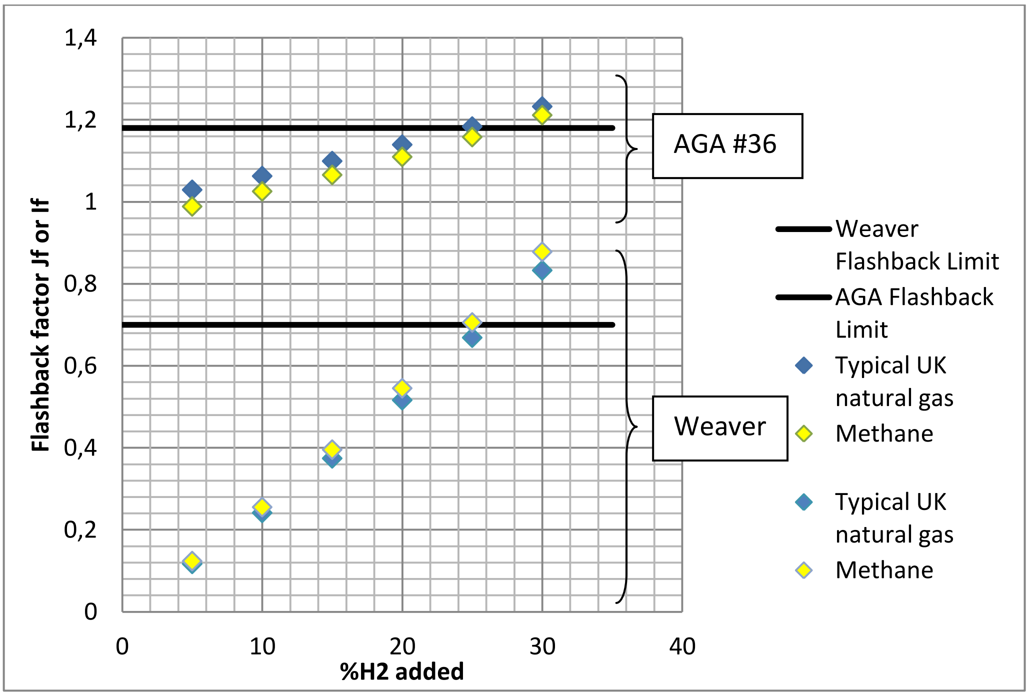

Figure 6 Comparison flashback indices

3.4 Dutton diagram

The Dutton diagram is a method to compare the interchangeability of gases; it was proposed by Dutton for British Gas. The idea was that gas mixtures should be compared on the basis of their composition. Because natural gas can consist of more than twenty components, a simplified or equivalent composition is used for comparison [9]. In the method, gas mixtures are decomposed into an equivalent mixture which only consists of CH_4, C_3H_8, N_2 and H_2. The hydrocarbons are replaced by an equivalent amount of methane and propane in such a way that the carbon content is the same. The nitrogen component is used to obtain the same Wobbe Index as the original gas. As with the AGA and Weaver interchangeability methods limits are based on experiments with household appliances.

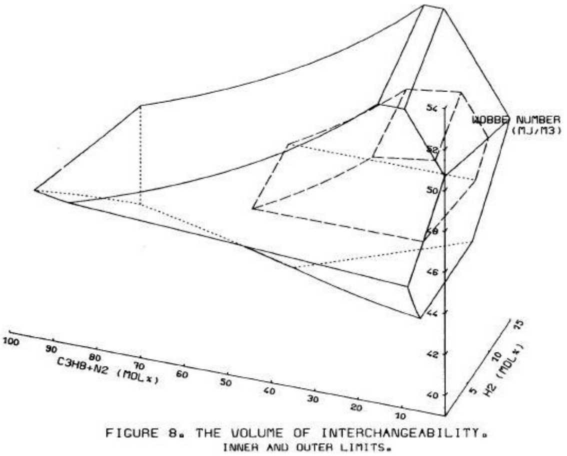

Figure 7 3D Dutton diagram

The diagram is three dimensional, with the Wobbe Index on the vertical axis, the amount of hydrogen on the depth axis and the sum of the equivalent amount of nitrogen and propane on the horizontal axis. The acceptable mixtures are bounded by limitations with respect to the lifting index (LI), soothing index (SI) and incomplete combustion (ICF). See Figure 7 to get a general impression of the 3D Dutton diagram.

In most cases the hydrogen dimension is dropped, because usually there is no or negligibly small amounts of hydrogen in the gas and a two dimensional diagram is presented. However, for the current research the hydrogen dimension is of great interest.

3.4.1 Dutton indices

Based on the experiments Dutton has derived formulas to calculate the indices. The interchangeability volume can be calculated with the following formulas (5-7) [7]. When the hydrogen fraction is dropped equations (6) and (7) are equal to the GS(M)R equations [1].

$$LI = 3.25 - tan^{-1}\big(C\,(0.122 + 0.0009H_2)\big)\,, \tag{5}$$

$$with\; C = WN - 36.8 - 0.019PN + (0.775 - 0.118PN^{1/3})H_2$$

$$ICF = \frac{WN - 50.73 + 0.03PN}{1.56} - \,0.01H_2 \tag{6}$$

$$SI = 0.896tan^{-1}(0.0255C_3H_8 - \,0.0233N_2 - \,0.0091H_2 + \,0.617) \tag{7}$$

PN is the total mole fraction of $C_3H_8 + N_2$ in the equivalent mixture calculated as described previously, WN is the Wobbe Index and H_2, C_3H_8 and N_2 the corresponding mole fractions in the equivalent mixture.

When the limits LI ≤ 1.16, ICF ≤ 0.48 and SI ≤ 0.60 are applied the Dutton diagram's normal volume is obtained, in emergencies an increase in the spread of Wobbe indices is allowed. The hydrogen dimension limits are 10%vol for normal operation and 15%vol in emergencies.

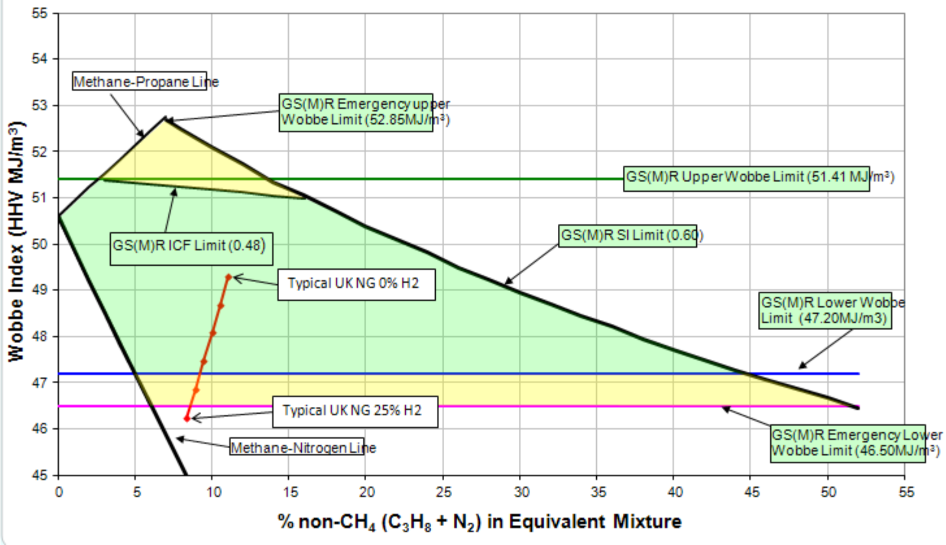

Figure 8 2D Dutton diagram

The effect of adding hydrogen (in 5% steps) to a natural gas is shown in Figure 8 above in the 2D Dutton plot; the hydrogen axis is dropped in this examination. The limiting value is the lower Wobbe Index; based on that about 17% hydrogen can be added without exceeding this limit. This is more than is allowed by Dutton's hydrogen limit, so the amount of hydrogen will be set by the normal hydrogen limit.

3.5 Multiple index interchangeability method limitations

The above mentioned methods of determining the interchangeability of gases have in common that they have the same global limitations. That is the derivation and scalability of the limits and the reference gas used. The limiting values are based on the results of many experiments done in a laboratory and a fit is added to predict the performance. It is possible that the limit suggests that there is no problem, but during operation there are problems.

The other problem is the scalability of the predictions and limits to equipment other than domestic appliances. The interchangeability predictions are based on experiments executed on appliances with combustion systems operating at approximately ambient temperature and pressure. They were not designed to predict the performance of combustion systems that operate at elevated temperature and pressure, such as gas turbines. To predict the performance at higher pressures and/or temperatures the formulas have to be adapted.

For a simple mixture of methane and hydrogen it is possible to calculate all the Weaver flame speed factors at a higher pressure or temperature, but for the other components present in natural gas there is less information on how their behaviour changes. By adapting the expressions they are stretched to and possibly beyond their limitations, so other methods have to be used to predict the performance under gas turbine operating conditions.

The chosen reference gas influences the interchangeability. A gas with a higher Wobbe Index allows for a greater increase of the Wobbe Index than a gas with a lower index. To determine the interchangeability it is important to know what gas will be received so that a good reference gas can be chosen for the comparison. As mentioned before the gas supply in the future will be less certain, there will be more fluctuations in composition, making it hard to choose a good reference gas.

4 Literature review

This chapter will look in more detail at the effects of hydrogen addition to natural gas. A change in fuel composition affects every aspect of combustion, such as flame speed, combustion dynamics and emissions. Due to the high reactivity of hydrogen and increased flame speed, flashback has been specifically investigated. The understanding gained in this chapter will be used as starting point for the analysis of the impact on E.ON's gas turbines later in the report.

These four categories are still very broad and therefore these are divided into subcategories to get a clearer view of what has to be done. The flame speed section is split into laminar and turbulent flame speed parts. The emissions section focuses only on the most important emissions, namely CO and NO_x. The combustion dynamics section focuses on the turbulent source term and a flame transfer function type of analysis. The flashback category focuses only on the main flashback mechanisms, combustion induced vortex breakdown and wall boundary layer flashback.

All these effects depend on the selected operating conditions; temperature, pressure and equivalence ratio. The equivalence ratio (ϕ), sometimes called the fuel-air equivalence ratio, is the ratio of the fuel/oxidiser over the fuel/oxidiser ratio at stoichiometric conditions. Stoichiometric combustion is the complete combustion of the fuel and air, with no fresh gas or air left. The equivalence ratio can be calculated using equation (8).

$$\phi = EQR = \frac{\frac{\dot{m}_{fuel}}{\dot{m}_{oxidiser}}}{\left(\frac{\dot{m}_{fuel}}{\dot{m}_{oxidiser}}\right)_{stoichiometric}} \tag{8}$$

The load of the gas turbine is omitted at the moment as this is not necessary to know to get a general understanding of the impact of hydrogen. Therefore a representative range of equivalence ratios will be used to estimate the effects of a load change. The equivalence ratio considered during normal continuous operation ranges from 0.3 to 0.5.

4.1 Laminar flame speed

Different researchers have investigated how the flame speed of natural gas changes when hydrogen is added. Some researchers replaced the natural gas by methane to simplify the experiments; the justification is that methane is the major component of natural gas. The experimental results are often compared to the laminar flame speed calculated by using the GRI 3.0 mechanism in CHEMKIN, sometimes other reaction mechanisms and programs are used.

Firstly a general description of the methane-hydrogen fuel mixture is given, followed by the comparison of the various correlations that have been produced by the difference researchers. Finally a correlation will be chosen that best describes the laminar flame speed.

4.1.1 Laminar flame speed regimes

When a methane-hydrogen mixture is burned there can be three regions defined depending on the hydrogen content [10]. Region I is from 0-50%vol, region II is from 50-90%vol and region III is from 90-100%vol hydrogen addition. In the regions I and III there is a linear relation between the hydrogen content and the flame speed. Region II serves as a transitional region. The regimes are sketched in the Figure 9 below.

In this report the addition of hydrogen up to 20%vol is considered, therefore all the results can be categorized as region I. On the basis of this short analysis we expect that all the flame speeds show a linearly increasing trend.

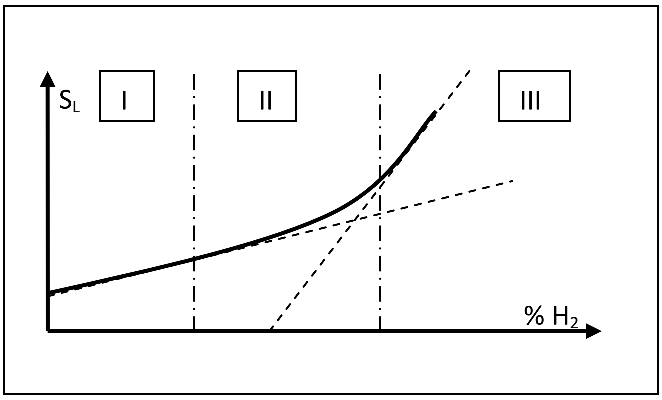

Figure 9 Flame speed regimes

4.1.2 Flame speed correlations

As mentioned before different researchers have produced relationships between the hydrogen content in a methane-hydrogen mixture and the laminar flame speed of the mixture; their correlations are shown below. The quality of the formulas that have been proposed differs with laminar flame speed regime, though only regime I will be investigated.

Yu et al [11] was one of the first that produced a relation between laminar flame speed, hydrogen content and equivalence ratio. In his relation the flame speed is related to the effective fuel-air ratio (ϕ_F) and the relative amount of hydrogen addition (R_H). It is necessary to know the hydrogen, fuel and air mole fractions for the calculations. The flame speed can be calculated by the relation (9).

$$S_L(\varphi, R_H) \cong S_{L0}(\varphi = \varphi_F) + \ 83\ R_H \ [\frac{cm}{s}] \qquad \text{Yu} \qquad (9)$$

S_{L0} is the flame speed with no hydrogen added. It is assumed the hydrogen oxidises completely, because it is present in small amounts and has a high reactivity, so less oxidiser is available for the methane, this is captured in the effective fuel-air ratio. This relation fitted well to the experiments conducted by them for both methane and propane mixtures.

Di Sarli et al [10] produced a relationship to predict the laminar flame speed that describes the effect of a broad range of hydrogen addition, i.e. they presented a relation that satisfies more than one of the above regimes. They came up with a Le Chatelier's Rule-like formula which depends on the mole fraction of hydrogen (x_{H2}) and the fuel-air ratio (ϕ) and the flame speed of the pure components (S_L). Shelil [12] proposed a relation that shows some similarity. His relation looks similar to the denominator of equation (10); this relation is not used in this report.

$$S_L(\varphi, x_{H_2}) = \frac{1}{x_{H_2}/S_{L_{H2}}(\varphi)\ + (1 - x_{H_2})/S_{L_{CH4}}(\varphi)} \qquad \text{Di Sarli} \qquad (10)$$

Di Sarli has validated his relation with calculations done with CHEMKIN. The formula shows good resemblance with respect to the calculations for lean and stoichiometric and the first part of rich mixtures for standard conditions and conditions with an elevated pressure and temperature.

Bougrine et al [13] also proposed a formula to calculate the laminar flame speed. He developed a complex formula that needs as input the hydrogen percentage (α), equivalence ratio (ϕ), inert mass fraction (Y_{res}^{u}), temperature (T) and pressure (P), where P^0 and T^0 denote the reference conditions. This formula (11) can predict the flame velocity for many conditions at the cost of additional complexity.

$$U_l(\alpha,\varphi,Y_{res}^u,T,P) = U_l^o(\alpha,\varphi)\cdot\left(\frac{T^u}{T^o}\right)^{\alpha_T}\cdot\left(\frac{P}{P^o}\right)^{\alpha_P}\cdot(1-\alpha_{res}f(Y_{res}^u)) \qquad \text{Bougrine} \qquad (11)$$

Except for the pressure and temperature all factors need to be calculated separately. The expressions and constants needed to calculate the laminar flame speed can be found in Appendix I. The formula is validated with calculations done with CHEMKIN and the GRI 3.0 scheme and showed good resemblance. The formula is validated for 1-110 bar, 300-950 K and 0.6-1.3 ϕ and 0 – 100% H_2.

Halter et al [14] did experiments up to 20% hydrogen at atmospheric and elevated pressures and compared the results with calculations performed with CHEMKIN. The experimental results compared well to the numerical results, although the latter had globally overestimated the results. Halter also compared the atmospheric results with the results of Yu and he found that the difference between them was caused by the experimental set-up used.

4.1.3 Comparison of the laminar flame speeds at standard conditions

The flame speeds of hydrogen-methane mixtures plotted in Figure 10 are all calculated or measured at standard conditions, i.e. 1 atmosphere and 298 K. For the relation of Yu the reference flame speed is needed, this is obtained from his measurements. For the Di Sarli relation the flame speeds of the pure components are needed, these are obtained from his calculations. The Bougrine relationship takes into account amount of diluents, but this is not needed for the methane hydrogen mixtures considered here.

All results show the same trend, a steady increase in flame speed with an increase in hydrogen content, just as predicted in regime I in Figure 9. There is a clear separation of the results into two sets; the Yu and Di Sarli results are very comparable, as are the results from Halter and Bougrine. As pointed out by Halter the results of Yu are an overestimation of the actual flame speed. Because the results of Di Sarli show a good resemblance with Yu his results are therefore also overestimating the flame speed.

The results of Halter and Bougrine are about the same and seem to be a good representation of the actual flame speed. Indicative experimental data available to E.ON, but yet to be verified or published tends to support the selection of the Halter and Bourgrine results.

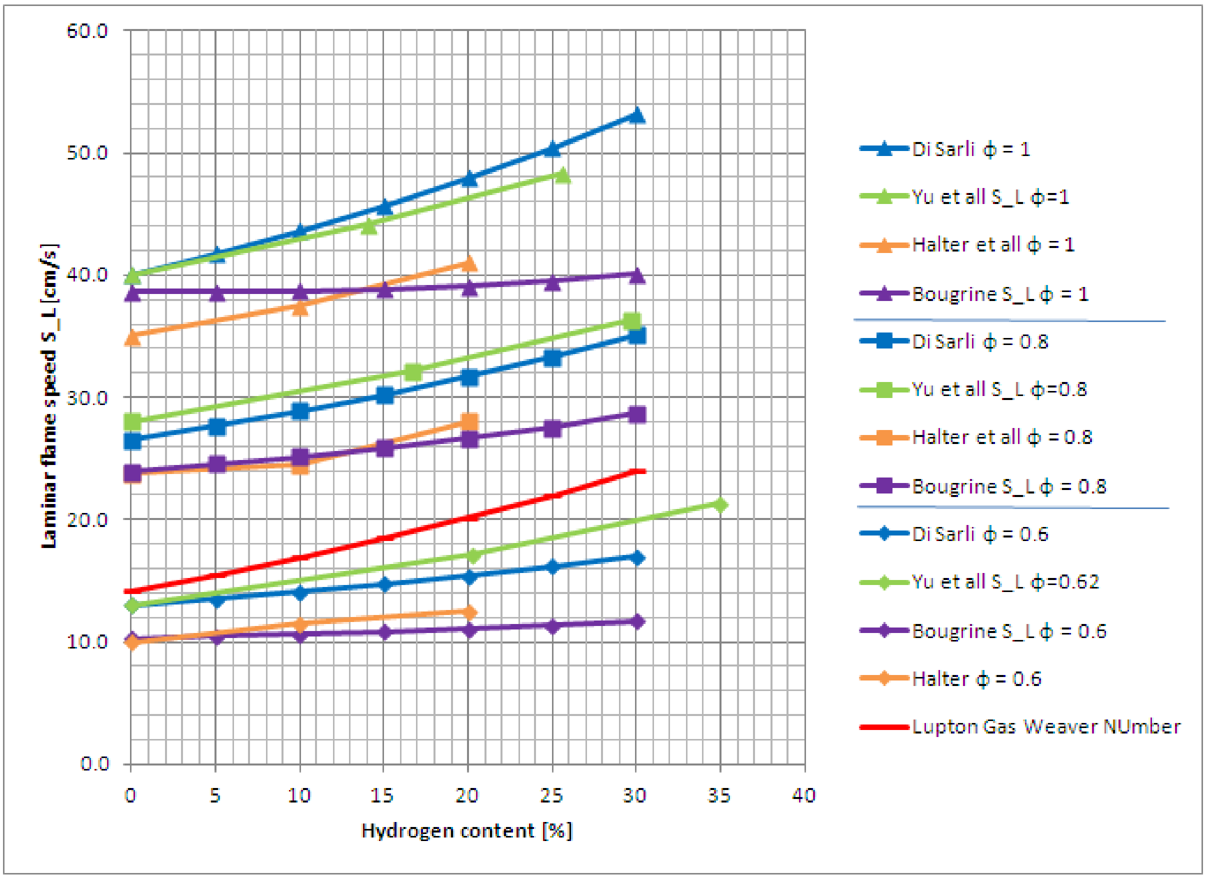

Figure 10 Laminar flame speed comparison at normal conditions

In Figure 10 is also the Weaver number, Weaver flame speed factor, added because there was the idea that this factor may be a good description for the flame speed of a methane/natural gas-hydrogen fuel mixture. Weaver assumed that there would be a complete (stoichiometric) combustion of the fuel mixture, the increasing of the laminar flame speed is represented well, however the magnitude of the flame speed is wrong. Furthermore, it would require a lot of work to adapt the Weaver correlation to equivalence ratios other than one. Therefore the idea of the Weaver flame speed factor describing the change of the laminar flame speed will not be pursued.

4.1.4 Comparison of the laminar flame speed at high pressure and temperature

The previous flame speeds were calculated at normal atmospheric conditions, but this is not representative of the operating conditions of gas turbines. In Figure 11 the Bougrine flame speeds are compared to those calculated by Brower [16] with CHEMKIN and an in-house developed reaction mechanism for a hydrogen-methane mixture. The equivalence ratio that Brower used was smaller than one, its exact value is unknown, based on the results it is probably close to one, further are the results based on different reaction mechanisms. By comparing Figure 10 and Figure 11, one can see that the increase in laminar flame speed is lower at gas turbine conditions, but is still a more or less linear increase.

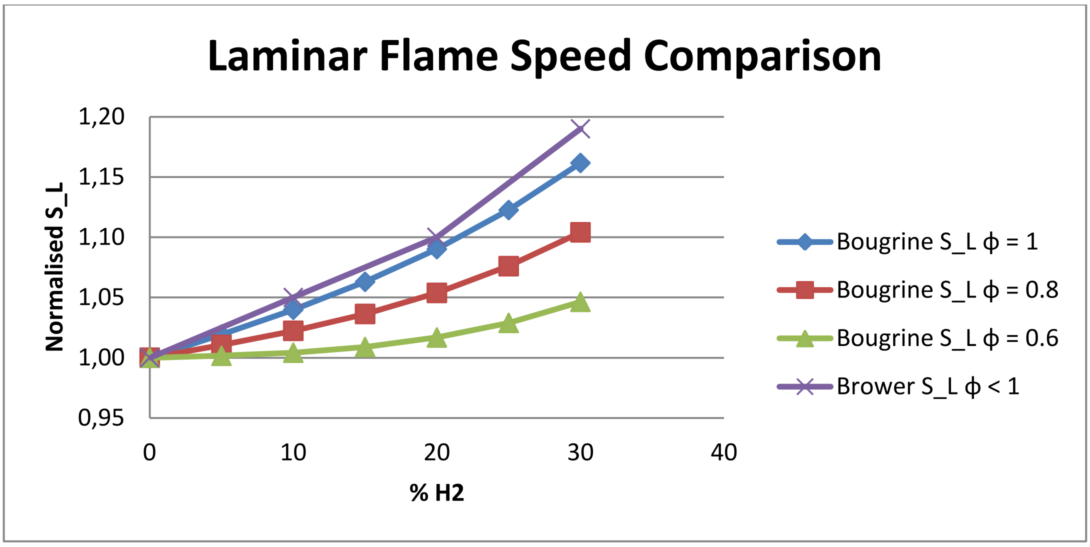

Figure 11 Brower and Bougrine flame speed at 25 atm and 480°C

The Bougrine correlation is also compared with flame speed data from DLR to investigate the performance at high temperatures and pressures at low equivalence ratios. DLR calculated the laminar flame speed with CHEMKIN and an in-house developed reaction mechanism, which is a combination of different reaction mechanisms [17]. The results are plotted in Figure 12 for two scenarios. The Bougrine relation shows distinctly different characteristics at its lower limit of stated validity (ϕ=0.6). This can be seen as it is not steadily increasing as expected.

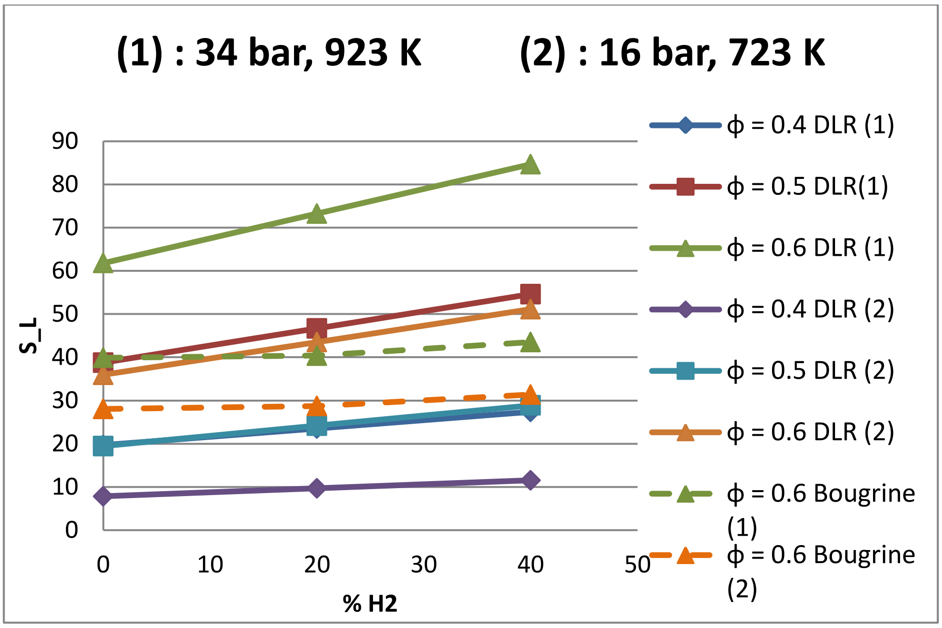

Figure 12 DLR and Bougrine flame speed

Compared to the DLR results, Bougrine is under predicting the flame speed for the lean mixtures. This is probably caused by the fit that is used in the formula. The Bougrine formula is a useful correlation for the laminar flame speeds, but one has to keep in mind its limitations. None of the above equations is validated for gas turbine conditions with equivalence ratios lower than 0.6. To get the required information, simulations will be carried out in CHEMKIN PREMIX. For these results see Sections 6.1.3 and 6.1.4.

4.2 Turbulent Flame speed

In gas turbine combustion systems the flow is turbulent, so there will be turbulent combustion, thus the turbulent flame speed is likely to be more relevant than the laminar flame speed. The turbulent flame speed differs from the laminar flame speed in magnitude and driving forces. The turbulence of the flow affects the flame, this can be seen by the eye as the general appearance of the flame changes.

The turbulent flame speed is a major parameter in determining the flashback risk. This will be explained in more detail in Section 4.5, and so having information on the impact of hydrogen on the turbulent flame speed is of great value.

4.2.1 Estimating the turbulent flame speed

It is valuable to be able to estimate the turbulent flame speed, therefore many researchers have researched it and derived expressions for the calculation of the turbulent flame speed. In many of these expressions the turbulent flame speed is related to the laminar flame speed and the velocity fluctuations in the flow (level of turbulence). Sometimes parameters like the pressure, temperature, flame thickness and a length scale are added to the correlation. However there is not one equation that adequately describes the turbulent flame speed, so correlations to calculate the turbulent flame speed have to be chosen very wisely.

Generally used correlations for the flame speed are given below (12 and 13) [18, 19]; these equations may capture the turbulence effects in general, but they are limited. Equation (12) is a simplification of (13), but both forms are widely used to indicate the same. These two general correlations indicate that the turbulent flame speed equals the laminar flame speed plus a scaled amount of turbulence.

$$\frac{S_T}{S_L} = 1 + \frac{u'}{S_L} \tag{12}$$

$$\frac{S_T}{S_L} = 1 + C\left(\frac{u'}{S_L}\right)^n \tag{13}$$

Other correlations have been proposed by Bradley, Schelkin, Kobayashi [20], UCI-Parker Hannifin [21] and Daniele [22], these relations are give below in equations (14) to (18) respectively.

Equations (14) to (18) have a similar form to the basic equations (12) and (13). The complexity depends on the scaling that is applied to fit their data. They tend to indicate that the velocity fluctuations dominate the laminar flame speed, i.e. turbulence dominates over the chemistry.

$$\frac{S_T}{S_L} = 1.52\left(\frac{u'}{S_L}\right) \qquad \text{[Bradley]} \tag{14}$$

$$\frac{S_T}{S_L} = \left(1 + \left(2\frac{u'}{S_L}\right)^2\right)^{0.5} \qquad \text{[Schelkin]} \tag{15}$$

$$\frac{S_T}{S_L} = 2.9\left(\left(\frac{P}{P_0}\right)\left(\frac{u'}{S_L}\right)\right)^{0.38} \qquad \text{[Kobayashi]} \tag{16}$$

$$\frac{S_T}{S_L} = 5.04 \left(\frac{P}{P_0}\right)^{0.2} \left(\frac{u'}{S_L}\right)^{0.38}$$ [UCI and Parker-Hannifin] (17)

$$\frac{S_T}{S_L} = 337.45 \left(\frac{u'}{S_L}\right)^{0.63} \left(\frac{L_T}{\delta_L}\right)^{-0.37} \left(\frac{P}{P_R}\right)^{0.63} \left(\frac{T_0}{T_R}\right)^{-0.63}$$ [Daniele] (18)

Another way of describing the turbulent flame speed is by relating it to relevant dimensionless numbers, this approach is used by Lipatnikov and Chomiak [18]. The dimensionless groups used are the Damköhler (Da) number (19), which compares the turbulence and chemical timescales, the turbulent Reynolds (Re_t) number (20), which compares the inertial and the viscous forces, the Karlovitz (Ka) number (21), which compares the smallest length scale of the turbulence eddies and the laminar flame, and the Lewis (Le)number, which compares the heat and the mass diffusivity. Pr is the Prandtl number (22), which compares the diffusion of momentum and heat; it is assumed to be 1 [18]. Lipatnikov and Chomiak analysed different flame speed databases and their correlations are given in the equations (23) to (26), each is based on a different database.

$$Da = \frac{\tau_t}{\tau_c} \qquad \tau_c = \frac{\delta_L}{S_L} \approx \frac{a_u}{S_L^2} \qquad \tau_t = \frac{L}{u\prime} \tag{19}$$

$$Re_t = \frac{u' L_T}{\nu_u} \approx \frac{u' L_T}{a_u} \tag{20}$$

$$Ka = \frac{\sqrt{Re_t}}{Da} \tag{21}$$

$$\mathrm{Pr} = \frac{\nu}{\alpha} \approx 1 \tag{22}$$

$$S_t \approx u' Da^{0.2} Re_t^{-0.3}$$ [L&C 1] (23)

$$S_t \approx u' Ka^{-0.41}$$ [L&C 2] (24)

$$S_t \approx u'(Ka \cdot Le)^{-0.3}$$ [L&C 3] (25)

$$S_t = S_L + 0.62 u' Da^{1/4} Pr^{-1/4}$$ [L&C 4] (26)

Brower chooses to combine both methods [16] in formulating the turbulent flame speed. The Brower correlation is given in (27), the effective Lewis number Le^* is given in equation (28) for a methane-hydrogen fuel mixture.

$$\frac{S_T}{S_{L0}} = 1 + \frac{0.46}{e^{(Le-1)}} Re_t^{0.25} \left(\frac{u'}{S_{L0}}\right)^{0.3}$$ [Brower] (27)

$$\frac{1}{Le^*} = \frac{D^*}{\alpha} = \frac{x_{CH4} D_{CH4}}{\alpha} + \frac{x_{H2} D_{H2}}{\alpha} = \frac{x_{CH4}}{Le_{CH4}} + \frac{x_{H2}}{Le_{H2}} \tag{28}$$

In the above a binary (something-air) mass diffusion coefficient is used, not a multi-component one because of the dominance of air in the overall behaviour of the mixture.

4.2.2 Comparison of the turbulent flame speed at normal conditions

The first comparison that is made is at normal pressure and temperature, 1 atmosphere and 298K, and an equivalence ratio of 0.8.

For the comparison the above equations were used to generate the results given in Figure 13. Limited experimental data was available and the experimental data shown on the plot is indicative data available to E.ON, but yet to be verified and published and should be treated with caution.

The laminar flame speed needed is calculated with CHEMKIN, for these results see Section 6.1.4. As expected there is a spread in the results. This confirms that one has to choose the correlation for the turbulent flame speed wisely. For this set-up the UCI-Parker Hannifin correlation seems to be the best one, because the flame speeds are close to the experimental values and it predicts the slope quite well.

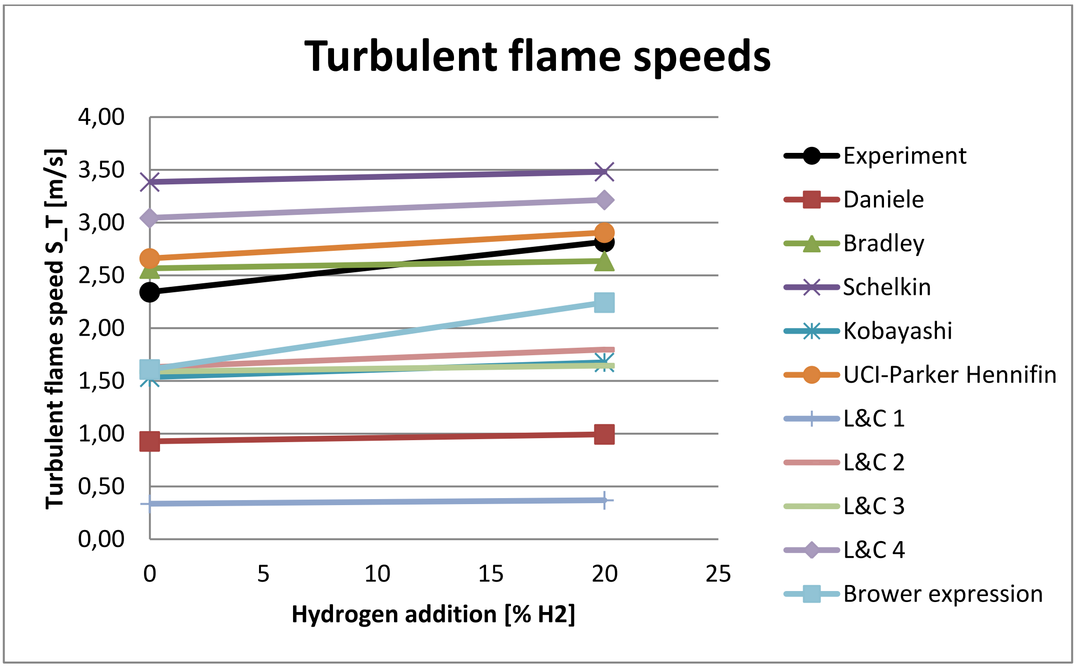

Figure 13 Turbulent flame speeds of methane-hydrogen air mixtures at normal conditions

4.2.3 Comparison of turbulent flame speeds at high pressure and temperature

The next comparison is done at conditions closer to typical gas turbine conditions. The inlet conditions are 14.4 bar and 673K. The equivalence ratios are 0.43 and 0.5. These conditions correspond to those used in experiments performed by Griebel et al [25] and the calculated values are compared to Griebel et al's experimental data. They also supplied detailed information about the flow and flame properties, therefore it is possible to make a double comparison.

The turbulent flame speeds are calculated with two methods, as is shown by the full and dashed lines. The first method, the full lines, uses all the flow and flame properties supplied by the paper to calculate the turbulent flame speeds. The second method, the dashed lines, uses flow and flame properties that are estimated or calculated with spreadsheets on basis of the NASA polynomials [23] and diffusion constants from Perry [24] and the laminar flame speed results from CHEMKIN as input for the turbulent flame speeds.

Both sets of results are shown in Figure 14. Here a spread is also clearly visible in the results of the turbulent flame speed prediction by the various calculations. The biggest difference is the change in performance of the correlations, i.e. a correlation that works well at normal conditions does not necessarily work at other (gas turbine) conditions.

Generally the results based purely on calculation agree well with those based on data from the paper [25] indicating that the method is reasonable. The relations that are the closest to the experimental values are the Lipatnikov and Chomiak number 2 and 3 and the Brower correlation.

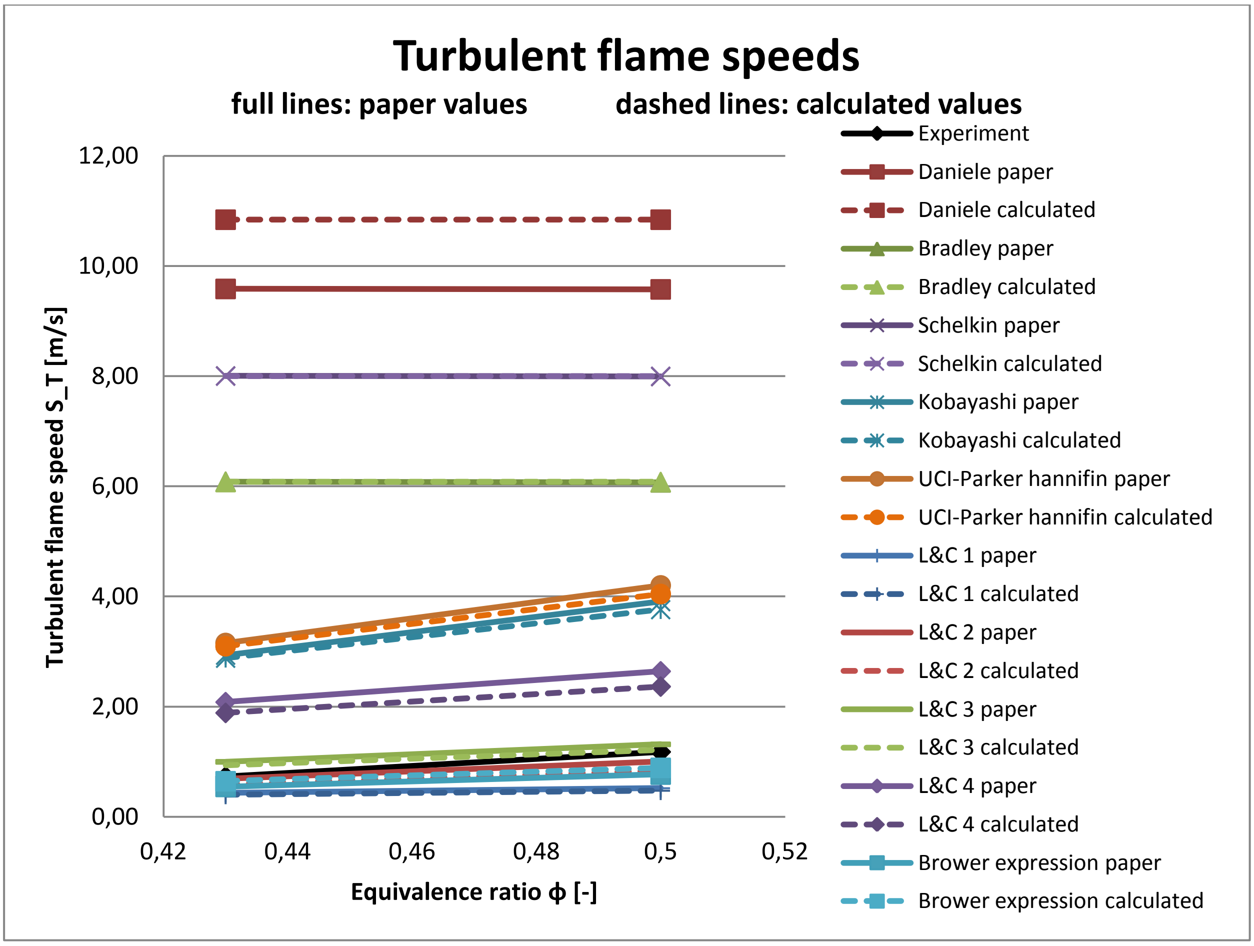

Figure 14 Turbulent flame speeds for methane air mixtures at gas turbine conditions (14.4 bar, 673K)

Figure 15 is zoomed in on the three correlations that predict the turbulent flame speed the best for this experiment. The best correlation depends on the method used, if the information from the paper is used the L&C 2 seems to be the best correlation and when our own information is used the L&C 3 seems to be the best correlation.

The three correlations in Figure 15 are chosen to calculate the turbulent flame speed as they show the best similarity with the experimental results. The lack of information makes a further selection of one correlation impossible. Further in this report, Section 5.2, a sensitivity analysis will be performed to investigate the robustness of these correlations and in Section 6.2 the correlations will be used to calculate the turbulent flame speed for the different gas turbines.

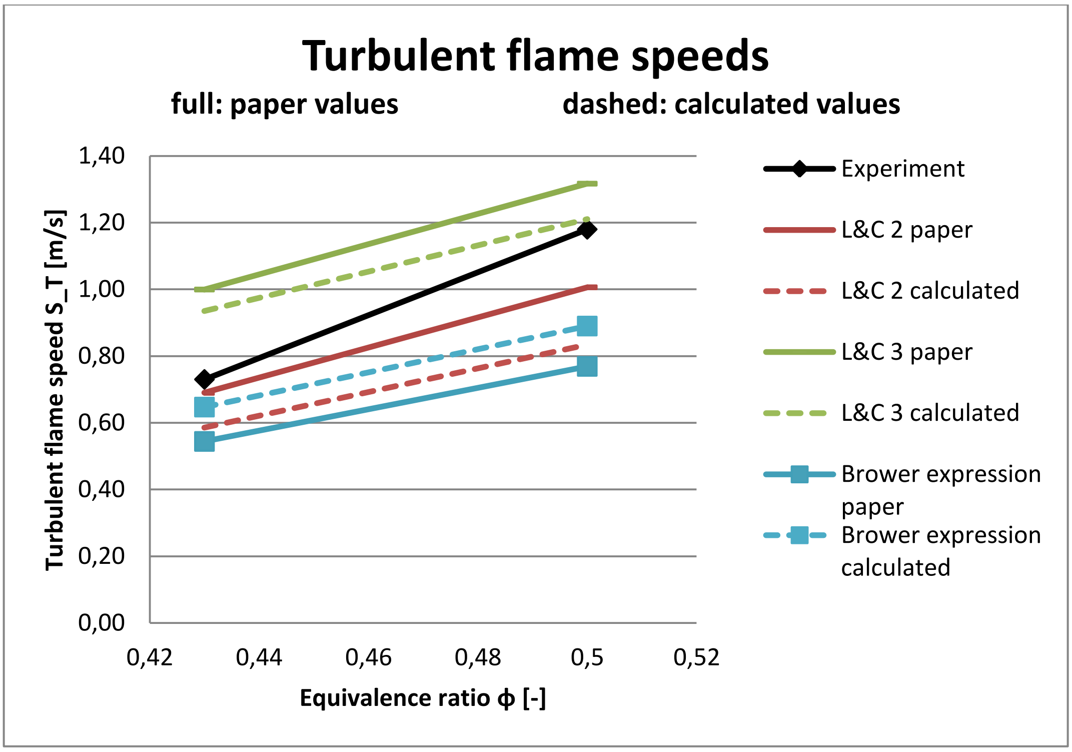

Figure 15 Turbulent flame speeds at gas turbine conditions (14.4 bar, 673K)

4.3 Emissions

The pollutant emissions produced are important due to their impact on the environment and public health; this is reflected in the tightening of regulations that state the maximum emission of pollutants [19]. In 2016, the Industrial Emissions Directive (IED) will define new emissions limits for gas turbines. This has driven improvements in gas turbine design and the operating strategy. In the literature there is some information about the change of the emissions as consequence of hydrogen addition, but as with the previous subjects there is little information available at gas turbine conditions.

The most important emissions are those of Oxides of Nitrogen (NO_x) and Carbon Monoxide (CO) in the exhaust gas. The NO_x, NO and NO_2, emissions can react further in the atmosphere causing smog and acid rain. The concern about CO is its toxicity, as it competes with O_2 to be absorbed into capillaries in the lungs. Other pollutant emissions are unburned hydrocarbons (UHCs) and oxides of sulphur (SO_x). The production of UHCs is influenced by the same factors as CO and thus methods of ensuring low CO also ensure low UHCs. SO_x is produced when there is sulphur present in the fuel. It can only be decreased by removing the sulphur from the fuel prior to combustion and normally pipeline natural gas has acceptably low sulphur content so that SO_X is not a significant issue.

In this report the focus will be on the CO and NO_x emissions. When only looking at these two emissions it is possible to define an optimum point of operation where the total emissions are minimal. Due to the opposite temperature dependence it is not normally possible to reduce them both indefinitely, therefore a trade off has to be made. Figure 18 illustrates this opposite temperature dependence, where LBO indicates the lean blow out limit. It also shows that the emission limits form the boundaries of an operating range.

4.3.1 Combustion concepts

For gas turbines there are two major combustion concepts: diffusion combustion and lean-premixed combustion. The difference between the two methods is the flame in the combustor and this will have an impact on the amount of emissions.

In Figure 16**Error! Reference source not found.** the two types are schematically presented [26]. In the diffusion combustor there is a separate injection of the fuel and air, the mixing of the fuel and combustion of it happens at the same time. The diffusion flame tends to burn at equivalence ratios close to one; creating a stable flame with a high flame temperature and high levels of $NO_{x,}$ the latter will be explained in more depth below.

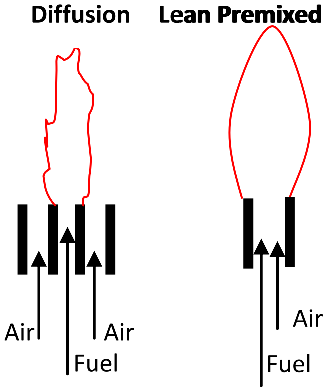

Figure 16 Flame Types

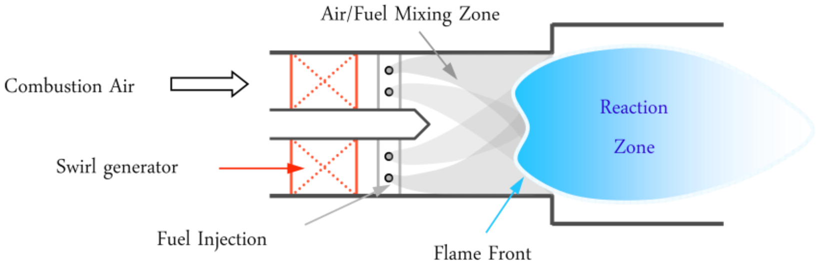

Figure 17 Basics of a lean premixed burner

In a lean premixed combustor the air and fuel are well mixed before they enter the combustor, shown in more detail in Figure 17 [3], this enables the flame to burn at low equivalence ratios producing lower flame temperatures and thus lower NOx levels than a diffusion flame. The disadvantage of lean premixed combustion is that its flame is less stable than a diffusion flame and is more sensitive to fluctuations in the flow and fuel quality, because the flame is close to the lean blow off limit. Nearly all modern gas turbines have a lean premixed combustor, so the focus will be on the emissions from this type.

4.3.2 Oxides of nitrogen

There are four mechanisms of NO formation within a flame. These are thermal NO, nitrous oxide mechanism, prompt NO and fuel NO. The thermal NO formation is mainly dominated by the flame temperature and it becomes most significant at temperatures above 1800- 1850 K, the Zeldovich limit. In the nitrous oxide mechanism NO is produced by the oxidation of N_2O. The N_2O is formed by the reaction of nitrogen and oxygen in the presence of a third molecule, acting as an intermediate. The prompt NO is formed by a reaction between the hydrocarbons of the fuel and the N_2 of the air to form HCN, which reacts further to NO. Fuel NO is caused by the combustion of nitrogen containing compounds in the fuel. In natural gas there is no chemically bound nitrogen ruling this mechanism out. Which of these mechanisms is dominant depends on the temperature and equivalence ratio.

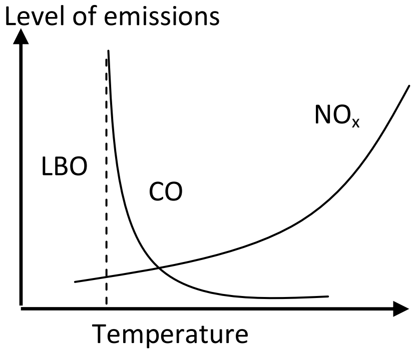

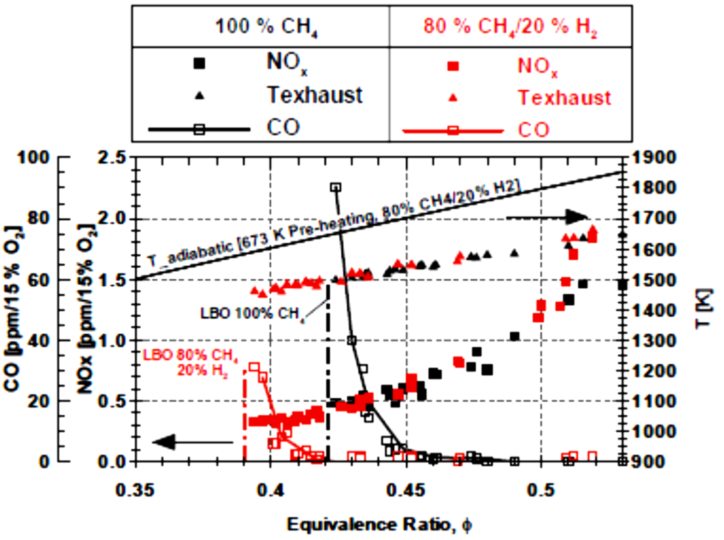

Figure 18 Global temperature dependence of emissions

Figure 19 Effect of H_2 enrichment of the emissions [28]

To minimise the NO_x levels in gas turbines, the fuel and air are mixed well before combustion to create an even fuel distribution and thus an even temperature distribution. An advantage of hydrogen is it lowers the lean blow off limit [27], enabling one to use lower equivalence ratios and produce less NO_x while maintaining the same level of CO; this is demonstrated by Griebel et al [28]. They showed (Figure 19) that at low equivalence ratios ($\phi \leq 0.5$) the NO_x formation is independent of the hydrogen content, indicating that there is no chemical enhancement of the NO_x formation due to hydrogen addition, leaving the flame temperature as main indicator of the NO_x formation.

Years ago a General Electric designed MS9001E DLN-1gas turbine was adapted to run on a natural gas blended with hydrogen, supplied by a local chemical plant [29]. The gas turbine was equipped with a DLN-1 combustion system, which is one of the earliest lean premixed systems. Hydrogen was added up to 12%vol at base load and 18%vol at part load. The results indicated that the NOx was not affected by the hydrogen, the change in emissions was in the noise of the tests, confirming that hydrogen does not chemically enhance the NO_x formation.

4.3.3 Carbon monoxide

The level of CO depends on the degree of combustion; when there is complete combustion there is no CO and lowering the degree of combustion causes an increase in CO due to the incomplete oxidation of CO to CO_2. This explains the sharp increase of CO emissions when the lean blowout (LBO) limit is approached [28]. The reaction time increases due to low burning rates and temperatures at lean mixtures combined with the increase in the likelihood of local extinction. In Figure 19 the results from Griebel et al illustrate the impact on emissions mentioned above. Further, the above mentioned operating window is shown and how it is affected by hydrogen addition.

The results from the measurements on the MS9001E gas turbine are less distinct than those of Griebel et al. On basis of the results shown in the paper it is hard to identify a trend. The addition of hydrogen tends to decrease the CO emissions, although this is difficult to identify in their results due to the noise of the data.

4.4 Combustion Dynamics

Combustion noise arises due to the combustion in the combustor. Noise is generated by turbulent flow noise and other flow effects and this may be amplified by the expansion of gas inside the flame, causing an expansion of the surrounding gas, creating a pressure (sound) wave. Variations in heat release within the flame may also contribute. This type of noise tends to be broadband in nature.

However, if the combustion noise is in phase with the heat release of the flame then acoustic feedback may occur resulting in high amplitude pressure oscillations. This type of noise is typically at a single fundamental frequency and related harmonics.

When the amplitude of these oscillations becomes too large they can reduce the operational life of the gas turbine and when the frequency equals one of the natural frequencies of the combustor or one of the combustion components the effect may be even more disastrous. Figure 20 shows the impact of severe combustion dynamics [3, 30]; the liner cap and mixing tubes are destroyed. This has been an issue for all gas turbine manufacturers and there is a wide range of names for the phenomenon including dynamics, pulsations, humming and screech.

Figure 20 Impact of severe combustion dynamics: [left] new component [right] damaged component

Due to the change in fuel reactivity when hydrogen is added the heat release of the flame may be changed, potentially changing the combustion dynamics.

Experiments conducted tend to indicate that hydrogen has an impact on the combustion dynamics. Tuncer et al [24] noticed a change in dominant frequency when hydrogen was added, this shift takes place at about 20%vol hydrogen addition. It should be noted that these experiments were performed at normal temperature and pressure and may not be relevant to gas turbine conditions. Also this could be due to effects such as change in flame position rather than a direct influence of hydrogen on the acoustic behaviour of the flame.

During the tests on the MS9001E the impact on the dynamics was also monitored [29]. The results showed that the hydrogen did not affect the magnitude of the combustion dynamics, neither did it change the switching point of the dominant frequency of the dynamics.

Another approach is to look at the theory that is used to describe combustion dynamics to estimate the impact of hydrogen addition. Considering representations of the acoustic source terms for the flame gives an indication of the noise generated directly within the flame. Alternatively considering the acoustic amplification properties of the flame (in this case represented by a simple flame transfer function) allows an assessment of the impact on feedback generated oscillations. These methods look at the driving forces behind the combustion dynamics and by estimating how these forces change an indication of the impact of hydrogen addition can be made.

4.4.1 Source term approach

The paper written by Kok [32] gives an explanation how the combustion dynamics are affected by a change in fuel quality. The combustion dynamics can be investigated by looking at the source term of the turbulent combustion process, the exact formulation of it depends on the model used, but they tend to depend on the laminar flame speed together with some other factors. In equation (29) the source term for the Burning Velocity Model is shown, which depends on the fresh gas density(ρ_u), the turbulent flame speed (S_T)and a reaction progress variable (c). The other parameters are a constant (C_f), the velocity fluctuations (u'), the turbulent length scale (L_t), the thermal diffusivity (α) and the laminar flame speed (S_L).

$$S = \rho_u S_T (\nabla c) \tag{29}$$

$$with\ S_T = C_f \left(\frac{u' L_t}{\alpha}\right)^{1/4} S_L^{1/2}$$

The change in laminar flame speed indicates the possible change in combustion dynamics, making it valuable to get a good understanding of the laminar flame speed.

4.4.2 Flame transfer function approach

The capability of a flame to amplify velocity fluctuations can be described by the flame transfer function [33]. Two important parameters of this transfer function are the fuel and air volume flow, or the volumetric expansion ratio and the time needed for the heat release. The change of this expansion ratio indicates the change of the amplification capabilities of the flame. The time needed for the heat release indicates the change in phase.

The expansion ratio (EPR) can be calculated with equation (30). It is a comparison of the volume of the gas before and after the flame, i.e. it compares the volume that the fresh gas has at the combustor inlet temperature and the volume of the combustion products at about the flame temperature. Further in this report, Section 6.1.6 and 6.3, calculations will be performed to investigate the change of this ratio when hydrogen is added to natural gas.

$$EPR = \frac{Volume\ combustion\ products}{Volume\ fresh\ gas} = \frac{V_{burned}}{V_{fresh}} \tag{30}$$

The time needed for heat release will be calculated in two ways, the first method looks at the total heat release and the second method looks at 80% of the heat release. The results from the CHEMKIN simulations will be used to calculate these times. More details about these methods can be found in Section 5.

4.5 Flashback


Figure 21 Flashback damage

Flashback is an unwanted combustion phenomenon, because of the damage it can do to the gas turbine burner. The damage that flashback can cause is shown in Figure 21 [30]. Experiments show that hydrogen tends to increase the likelihood of flashback to occur [12]. There is no single mechanism that causes flashback; there can be four different mechanisms identified that cause it [34, 35]. These mechanisms are: wall boundary layer flashback, turbulent flame propagation in the core flow, flashback due to instabilities and combustion induced vortex breakdown. After a general description of these mechanisms the two most likely mechanisms will be investigated in more depth.

4.5.1 General description of the flashback mechanisms

The most evident way of flashback is turbulent flame propagation through the core flow, and in this case the turbulent flame speed is higher than the mean flow velocity, therefore making it possible for the flame to move upstream. As mentioned earlier in the report the turbulent flame speed in general depends on the laminar flame speed and the velocity fluctuations. The laminar flame speed appears to be low in gas turbines and the velocity fluctuations are about 10-15% of the mean flow velocity, therefore it will be unlikely that this sort of flashback will occur.

Instabilities in the flow, like noise or pulsations, can cause the flame to move upstream. This flashback mechanism happens at high noise levels which are destructive to the machine making this mechanism unlikely to occur unless there is also a problem with combustion dynamics.

When the flame propagates upstream through the boundary layer, where the velocity is low, the flashback is called wall boundary layer flashback (WBLF). The flame can quench due to the cooling effect of the combustor wall. The description of the critical gradient depends on the type of boundary layer, laminar or turbulent. An uneven mixing of the fuel in the air may enhance this type of flashback.

When the flame propagates rapidly upstream along the centre axis of the burner at high speeds there is combustion induced vortex breakdown (CIVB) flashback. Burners with a centre body are less sensitive to this type flashback, because the aerodynamic effects of the centre body or central fuel lance enhance the flame stabilisation. Burners without centre body rely on an advanced aerodynamic design to create recirculation zones for flame stabilisation and these can be influenced by the collapse of the centre vortex.

The latter two mechanisms are the most likely to cause flashback in a gas turbine and can be described with the gradient and Konle model respectively. These two models will be explained in more detail in Section 5 and some basic predictions will be made.

5 Review of assessment tools/methods

In this section the different methods that will be used to investigate the effects of hydrogen addition will be explained. The CHEMKIN PREMIX package will be used to calculate the laminar flame speed of hydrogen-natural gas fuel mixtures, the concentration of the species involved in the reactions and the temperature profile will be used to calculate the time needed for heat release. The three turbulent flame speed correlations will be evaluated to see the impact of uncertainties in the prediction of the parameters on the predicted flame speed. The expansion ratio will be calculated assuming there is ideal combustion of the fuel mixture. The Konle and Gradient method will be investigated to predict the likelihood of flashback based on current flashback information.

5.1 CHEMKIN

The Available CHEMKIN [36] package contains the EQUIL and PREMIX functionalities. The EQUIL program calculates the equilibrium composition and temperature of a given mixture at a known initial temperature and pressure. The program does this by minimising the Gibbs free energy. The PREMIX program calculates the propagation of chemical reaction in a premixed ideal gas mixture. The program uses the governing equations to solve the temperature and species profiles in the flame. To simplify the computations there are some assumptions made in the program, the most important are about temperature losses and species transport.

The GRI 3.0 reaction scheme [42] is able to calculate reactions of hydrocarbons only up to propane (C_3H_8). This limits its usefulness for natural gas simulations as there are C4 and C5 hydrocarbons present in natural gas. This problem is solved by replacing the composition of natural gas by its Dutton equivalent composition, expressing it in CH_4, C_3H_8, N_2 and H_2.

The mechanism is validated for a certain range of conditions, shown in Table 4. The pressures that are investigated in this report are beyond the validated range (above 10 atm), therefore a short validation will be performed to check its validity and these results are shown further in the report in Section 6.1.1.

Parameter	Validated range
Temperature (hot gas)	$1000\ K \leq T \leq 2500\ K$
Pressure	$1.315*10^{-2}\ atm \leq P \leq 10\ atm$
Equivalence ratio	$0.1 \leq \phi \leq 5$

Table 4 Validated range of the GRI 3.0 mechanism

The simulations will be set up in such a manner that the heat input of the mixtures remains constant when hydrogen is added, because gas turbines are usually controlled by the heat input to the combustor or the firing temperature. This is done by changing the mole fractions of the fuel components till the target heat input is reached and the rest of the mixture is then made up by air.

By determining the molar fractions of the mixture in this way a change in equivalence ratio is caused, however the change in equivalence ratio was found to be negligibly small. The calculations are spread into three different categories, as shown in Table 5.

The categories describe typical base load operating conditions for the gas turbines at three E.ON power stations as mentioned earlier (Section 2.2.2). The set numbers and GT manufacturer will be used interchangeably to describe a set of results.

	Set 1	Set 2	Set 3
Power Station	Connah's Quay	Cottam Development Centre	Enfield
Gas Turbine	9FA	SGT5-4000F	GT26B
Manufacturer	General Electric	Siemens	Alstom
Pressure	15 bar	20 bar	30 bar
Temperature	400 °C 673 K	460 °C 733 K	550 °C 823 K
Equivalence ratio	0.3 - 0.5 Steps of 0.05	0.3 - 0.5 Steps of 0.05	0.3 - 0.5 Steps of 0.05
Hydrogen addition	0 - 20 %vol Steps of 5%vol	0 - 20 %vol Steps of 5%vol	0 - 20 %vol Steps of 5%vol

Table 5 Simulation parameters

5.1.1 Detailed description of PREMIX

The program [36] is capable of two types of calculations, a burner stabilised flame and a freely propagating flame [26, 37]. For the burner stabilised flame the temperature profile is known and a first flame can be computed, and is often used to calculate the species profiles in the flame. The freely propagating flame uses a first flame solution to investigate the influence of changing parameters, like pressure, temperature and equivalence ratio.

For the simulations in this report a freely propagating flame has been selected. When this flame type is chosen the program automatically assumes that the flame is steady and adiabatic to reduce the complexity of the governing equations. The governing equations are the mass conservation (continuity equation), species conservation and energy conservation. The reduced governing equations are shown below in respectively equations (31-33).

$$\rho u = constant = \rho_1 s_L \tag{31}$$

$$\frac{\partial}{\partial x}\left(\rho(u + V_k)Y_k\right) = \dot{\omega}_k \tag{32}$$

$$\rho C_p u \frac{\partial T}{\partial x} = \dot{\omega}'_T + \frac{\partial}{\partial x}\left(\lambda \frac{\partial T}{\partial x}\right) - \frac{\partial T}{\partial x}\left(\rho \sum_{k=1}^{N} C_{p,k} Y_k V_k\right) \tag{33}$$

Due to the steady state assumption the governing equations are now with respect to the reference frame of the flame, i.e. moving at S_L, thus the flame speed can be derived from the continuity equation. To 'close' this set of equations there is a expression needed for the reaction rate $\dot{\omega}_k$ and the diffusion velocities V_k. Often the Arrhenius law and Fick's law with a velocity correction are used respectively.

To solve this set of equations the program uses an iterative, Newton type, solver to solve the boundary value problem. Therefore the reactants and estimated products and a temperature profile have to be given as an initial guess for the solver. This is schematically represented in Figure 22 taken from the PREMIX manual [37]. Furthermore the temperature has to be specified at one point in the domain as an additional boundary condition, this is needed because the mass flow rate is an eigenvalue of the freely propagating flame simulation. The program calculates an estimate of the species profiles by assuming a fixed temperature in the domain. This estimate serves as input to the energy equation in the full calculation, which gives the final temperature and species profiles.

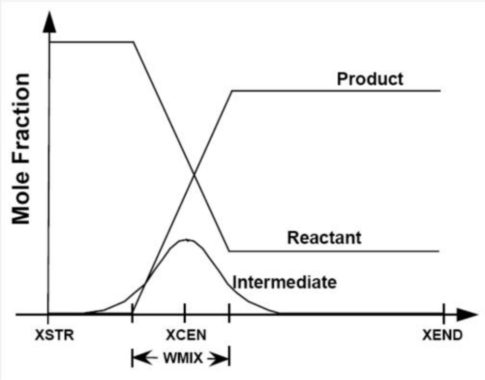

Figure 22 Basic configuration for the 1D premixed flame

Sometimes clever continuation techniques are used to calculate a new solution with a previous solution as starting estimate. This method can be useful when it is difficult to get the solver to converge to a solution. For the simulations in this report the temperature profile was estimated on the basis of the equilibrium temperature of the mixture and a visual fit to a given temperature profile; the latter is done to qualify the shape of the temperature profile. This method did not cause any problems with the convergence of the simulations making continuation techniques unnecessary.

5.1.2 Characteristic combustion time

For the assessment of the impact of hydrogen on the acoustic amplification properties of the flame, the information from PREMIX can also be used to calculate the characteristic combustion time; it is the time needed for the temperature to rise from the input temperature to final temperature. Two methods were used to evaluate the characteristic time; a maximum gradient method and a 10-90% temperature method, both methods will be explained below. Both methods are based on a time-temperature plot of the PREMIX results.

The maximum gradient method determines the time needed for the temperature to rise on the maximum temperature gradient with respect to the time in the flame. The time can be calculated with equation (34). To calculate the maximum gradient the mesh from the CHEMKIN results is used.

$$t = \frac{\Delta T}{\left.\frac{dT}{dt}\right|_{max}} \tag{34}$$

$$with\ \Delta T = T_{burnt\ gas} - T_{fresh\ gas}$$

This method is shown graphically in Figure 23 on the left. The maximum temperature gradient is used (dashed line) to describe the change from the low to the high temperature (solid line).

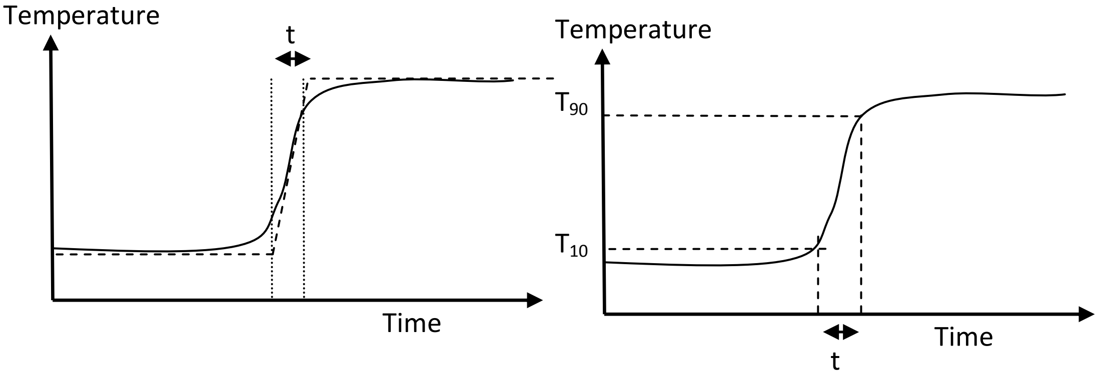

Figure 23 Maximum temperature gradient method (left) and the 10-90% method (right)

The 10-90% method determines the time needed for the temperature to increase from +10% of the fresh gas temperature to 90% of the final temperature. These two points can be calculated on the basis of the known start and final temperatures.The corresponding times are determined by processing the CHEMKIN results. The time is calculated with (35) and this method is shown graphically in Figure 23 on the right.

$$t = t(T_{90}) - t(T_{10}) \tag{35}$$

$$with \quad T_{10} = 1.1 \cdot T_{fresh\ gas} \qquad T_{90} = 0.9 \cdot T_{burned\ gas}$$

The first and last 10% of the heat release are not taken into account so that the effects of slow reactions at the start and end do not affect the results, because the combustion will be mostly affected by changes in the major heat release.

5.2 Turbulent flame speed correlation sensitivity

To calculate the turbulent flame speed various parameters need to be known and their accuracy determines the accuracy of the result. In the previous results, Section 4.2.3, the turbulent length scale, the velocity fluctuations and laminar flame speed were supplied by the researchers [25]. When the correlations are applied at different conditions, say to estimate the impact on different gas turbines, these parameters are likely to change. Due to the difficulty in determining these parameters a sensitivity analysis is performed to establish the required level of accuracy.

The velocity fluctuations are varied in three steps from the original value from the paper in each step the ‘level of uncertainty’ increases; the steps are +10%, +100% and +1000%. The last step indicates that the error is an order of magnitude. Also plotted will be the impact of these changes to different fuel compositions, fuels with 20%vol hydrogen and without hydrogen are used. This set up is used for all sensitivity analyses. The parameters used are shown in Table 6.

Parameter	Value	Change
Pressure	15 bar	0%
Temperature	673 K	0%
Mean flow velocity	35 m/s	0%
Velocity fluctuations	10% of U, 3.5 m/s	0%, +10%,+100%,+1000%
Turbulent length scale	1.18E-3 m	0%, +10%,+100%,+1000%
Laminar flame speed	Results from CHEMKIN	0%, +10%,+100%,+1000%

Table 6 Sensitivity analysis parameters

The results for the velocity fluctuations sensitivity with 0% hydrogen are shown in Figure 24 and Figure 25 below. In Figure 24 the results are shown only for the Brower correlation with 0% hydrogen, so the effects of increasing velocity fluctuations are clearly visible. In Figure 25 the results of all three correlations are shown.

The points with fluctuations increased by 10% coincide more or less with the points on the original line; the difference between them is a few percent. The points of 100% increase are a little above the line, the difference is about 40%. The points with that have been increased to 1000% of the original are significantly off the original values.

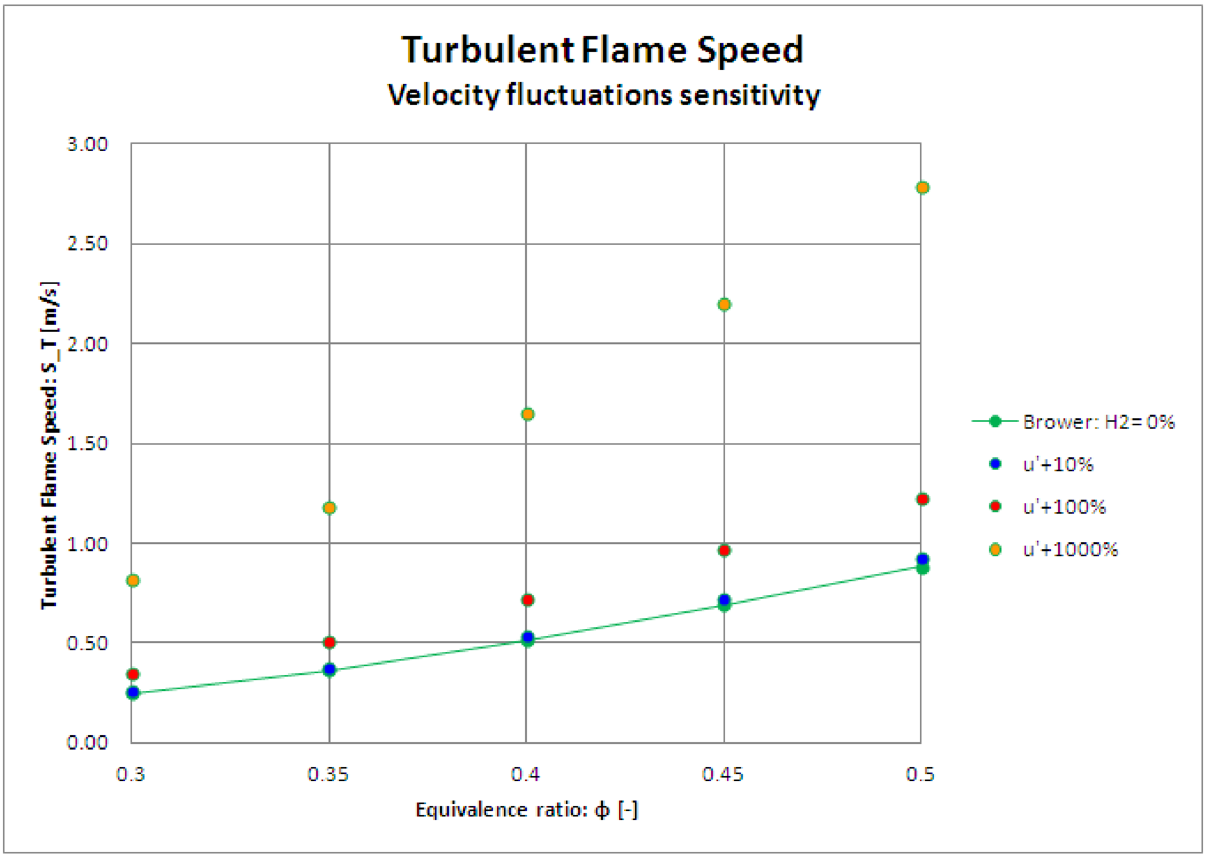

Figure 24 Sensitivity of the Brower correlation to velocity fluctuations: 0% Hydrogen

Figure 25 show that all the three correlations predict the same trend with increasing velocity fluctuations. The L&C 2 correlation is the least sensitive to hydrogen addition and the L&C 3 the most. The results with and without hydrogen show similar trends.

The results of the turbulent length scale analysis are shown in the Figure 26 and the results of the laminar flame speed in Figure 27. The results are very similar to results for the velocity fluctuation analysis. The points of 10% uncertainty coincide with the line and the points of +100% are offset a little, they are about 20% and about 60% larger respectively. The points of +1000% again change significantly.

When the results of both analyses are compared, the turbulent flame speed seems to be most sensitive to a change in the laminar flame speed. To produce estimates of the turbulent flame speed accurate values of laminar flame speed are needed, whereas estimates of turbulence intensity and length scale will often be sufficient, although the order of magnitude of these three parameters has to be known.

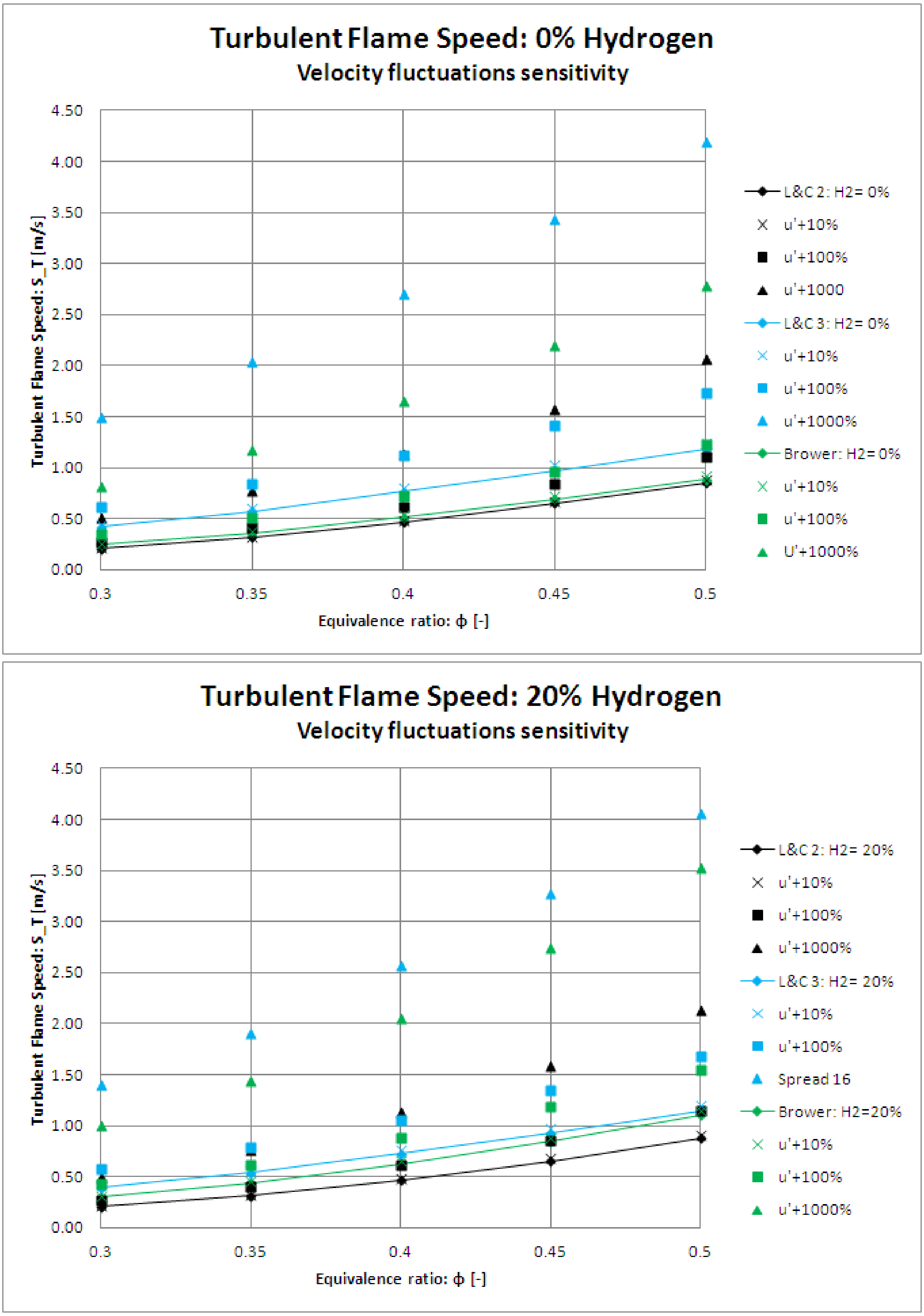

Figure 25 Sensitivity to Velocity Fluctuations: 0% [top] and 20% [bottom] Hydrogen

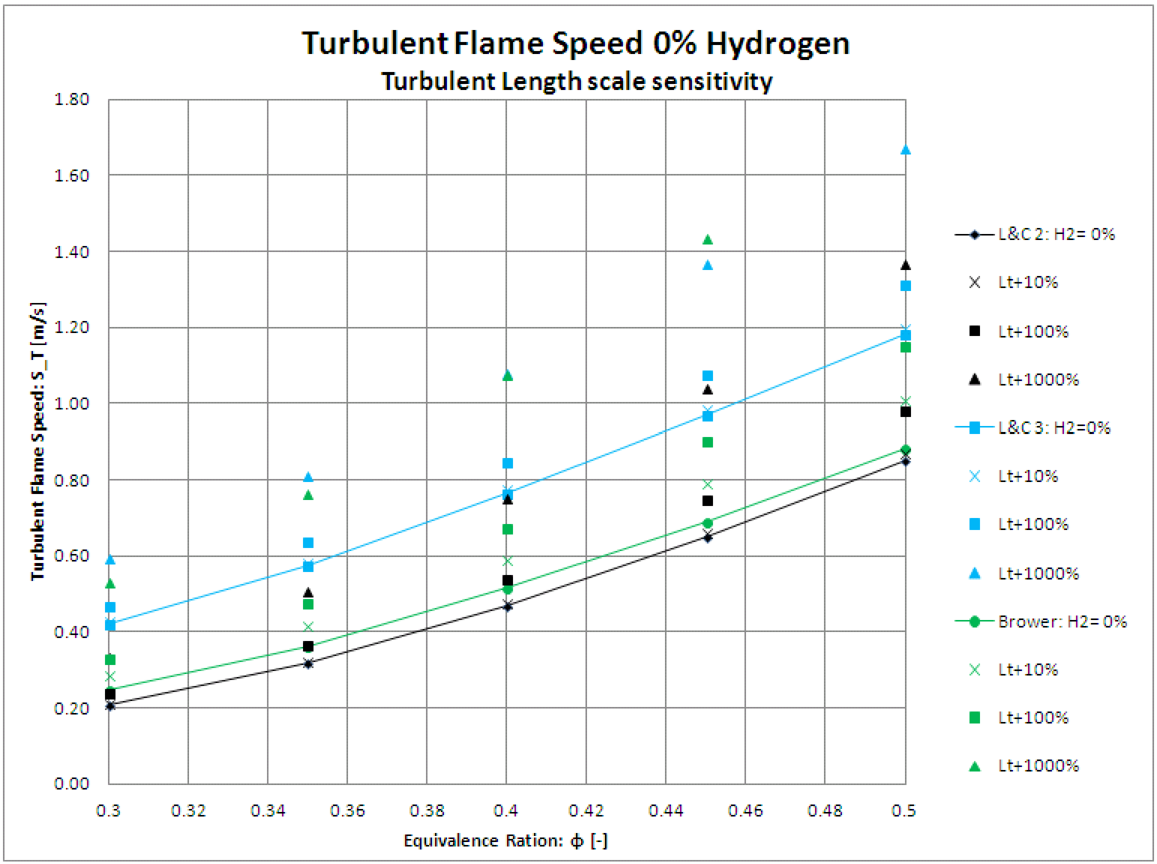

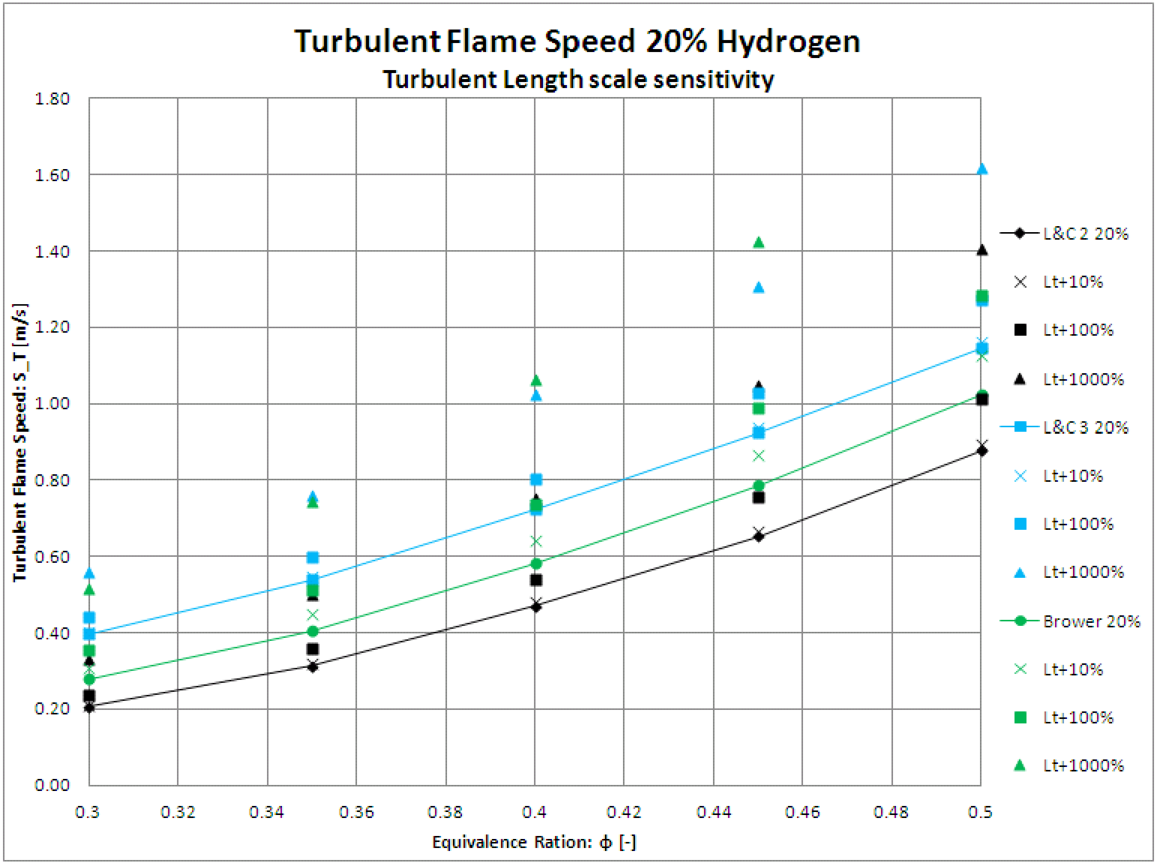

Figure 26 Sensitivity Turbulence Length Scale: 0% [top] and 20% [bottom] Hydrogen

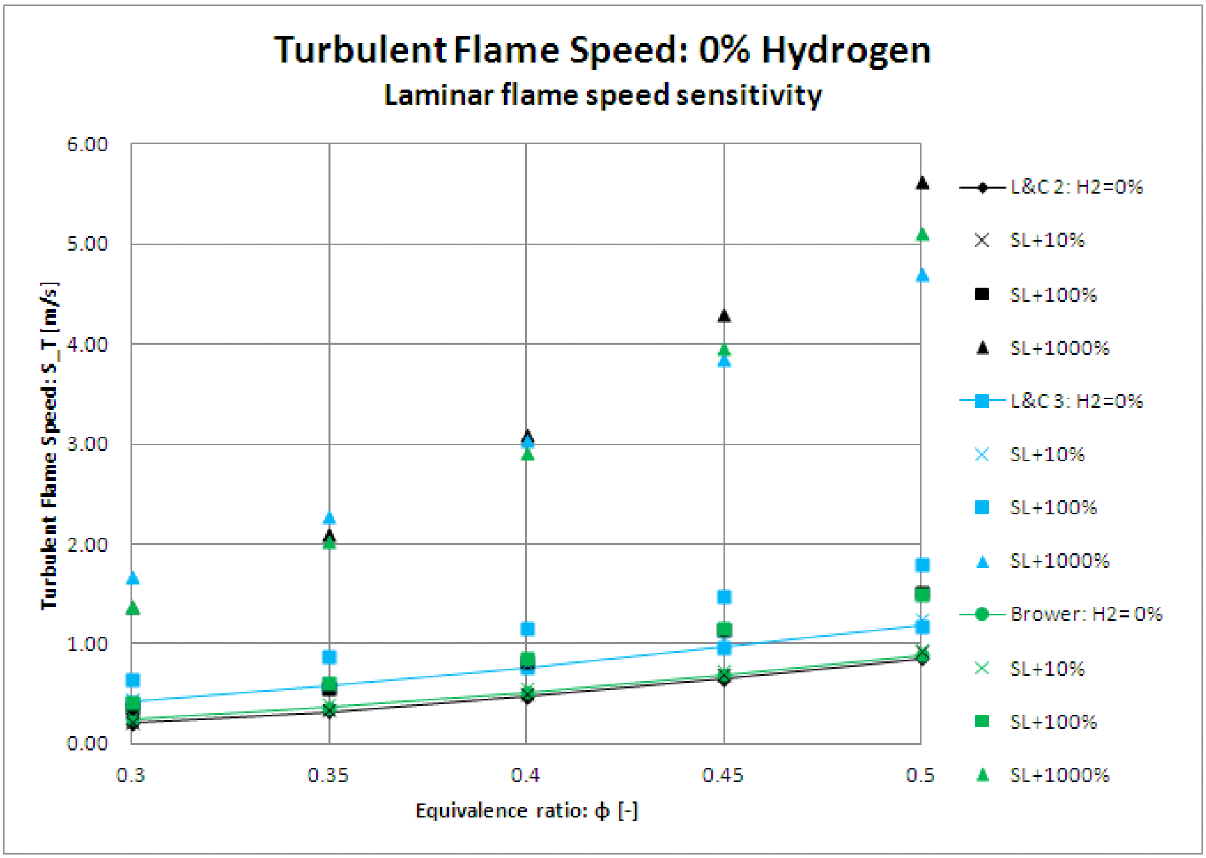

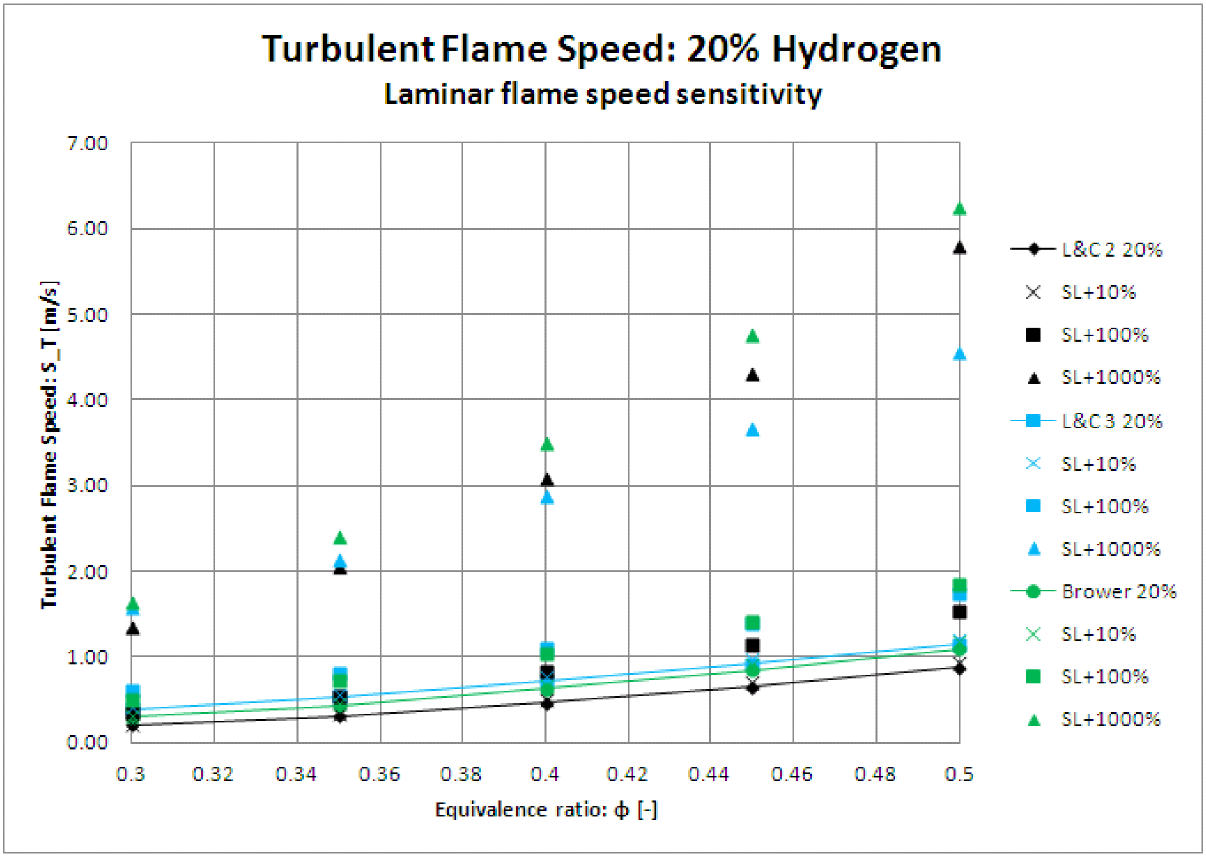

Figure 27 Sensitivity to Laminar flame speed: 0% [top] and 100% [bottom] Hydrogen

5.3 Volumetric expansion ratio

By investigating the change of the expansion ratio the change in amplification capabilities of the flame can be assessed. The approach taken in this report is based on a simple chemical scheme and the flame temperatures from the CHEMKIN simulations.

For the calculations, typical operating conditions of the Alstom GT26B will be used together with fuel and air flow data estimated from operational data at Enfield power station. These and other parameters of the calculation are given in Table 7.

	Fresh Gas	Burned Gas
Temperature	T = 823K	T = flame temperature depends on EQR
Pressure	P = 30 bar	P = 30 bar
Volume flow	Vair = 1.152 m3/s Vfuel depends on EQR and %vol H2	V = depending on EQR and %vol H2

Table 7 Expansion ratio calculation parameters

The ideal gas law (36) is used in two ways: to calculate the unknown moles in the fresh air from the given volume flow and the volume of the burned gas from the moles after the chemical reactions.

$$PV = nRT \tag{36}$$

$$with\ R = 8.314\ \left[\frac{J}{mol.K}\right], the\ universal\ gas\ constant$$

The moles in the fresh air are calculated with the ideal gas law. It is assumed that the combustion will be ideal and complete, there will be negligible NO_x and other products formed (for the purposes of this calculation), so it can be described with a simple one way reaction as in equation (37) below.

$$C_xH_y + \left(x + \frac{y}{4}\right) O_2 \rightarrow x\ CO_2 + \left(\frac{y}{2}\right) H_2O \tag{37}$$

Based on this ideal combustion the composition of the burned gas can be determined by taking into account the creation and depletion of species involved in the reaction in combination with the non reacting species. Based on this new composition at elevated temperature the volume can be calculated with the ideal gas law.

This calculation will be repeated for different levels of hydrogen addition to typical UK natural gas and at different equivalence ratios. When hydrogen is added to the fuel the heat input is kept constant by adapting the fuel volume flow; the shift in equivalence ratio is negligibly small.

5.4 Konle model for CIVB

The combustion induced vortex breakdown flashback can be reasonably described and predicted with the ‘Konle model’ [38,41]. The model is based on the comparison of the chemical and turbulent timescales. The model can predict the flashback behaviour at different operating points when one reference point, one recorded flashback, is known. The Konle model was introduced for flows with a moderate level of turbulence in the centre of the swirling flow. Equation (38) can be used to describe the model; here the most simplified form of the model is shown.

$$C_b = \frac{\tau_c}{\tau_t} = \frac{\bar{u}}{S_l} \tag{38}$$

The reference point is used to determine the model's constant C_b. This constant is used to predict flashback at other operating points. However this value of C_b is for a specific burner, fuel, temperature and pressure. This leaves the equivalence ratio as the only free parameter. For the analysis it is assumed that the behaviour of the fuel does not change significantly with hydrogen addition, so that the value of C_b can be used to investigate the impact of hydrogen addition.

There was a known flashback risk on the Alstom GT26A/B gas turbines and it is believed that changes in burner/combustor design resulted in significantly reduced flashback risk for the later ALSTOM GT26B machine. The estimated operating conditions of the two gas turbines are shown in Table 8 below. It has been assumed that the fundamental behaviour of the burner has not changed, but the design changes have resulted in a higher mean flow velocity. Design changes may also have changed other design features such as swirl number and fuel placement, but these have not been considered in this analysis because of lack of available detailed design data.

	GT 26 A/B	GT 26 B
Burner air flow	11.7 kg/s	14.625 kg/s
Burner fuel flow	0.233 kg/s	0.292 kg/s
Burner equivalence ratio	0.31	0.31
Mean flow velocity	35.35 m/s	49.39 m/s
Flashback likeliness	May flashback	Stable operation

Table 8 Gas turbine operating conditions

5.5 Gradient method for WBLF

The wall boundary layer flashback can be reasonably described with a critical gradient model [38]. This model is based on the Blasius wall friction concept for turbulent flows. When a flashback is recorded this gives information about the critical gradient and its value can be calculated with equation [39].

$$g = 0.03955 U^{7/4} d^{-1/4} \mu^{-3/4} \rho^{3/4} \tag{39}$$

$$g_{crit}^{*} = g_{crit} \left(\frac{T_{amb}}{T_{preheat}} \right)^{1.52} \quad and \quad g_{crit}^{**} = g_{crit}^{*} \left(\frac{P_{amb}}{P_{exp}} \right)^{1.35} \tag{40}$$

Measurements have been conducted by other researchers at different conditions therefore some scaling has to be applied to be able to compare the results to make the flashback prediction. The temperature and pressure scaling may be achieved by using equation (40). However the quality of the scaling varies, the temperature scaling seems to be reasonably good, but the pressure scaling is poor and problems are expected for scaling to gas turbine conditions [38]. The latter makes the model unsuited for the prediction of flashback in gas turbines, where the pressure in significantly increased. Therefore no results will be shown in this report for this method.

6 Analysis at gas turbine conditions

In this section the results will be presented that are obtained when the methods described previously are executed. Depending on the quality of the results they are presented for one or more of the three main gas turbine types. First the results from PREMIX are evaluated. Methods requiring certain CHEMKIN output are added here. It is followed by the results of the expansion ratio calculations and the Konle model.

6.1 PREMIX results

First the validation of the use of the GRI 3.0 reaction scheme will be presented. This is followed by the general and specific output. The general output section shows the capabilities of the program and gives an idea of how the main parameters change. The specific outputs are the laminar flame speed, emissions and characteristic burning time.

6.1.1 Validation of the use of reaction scheme

As identified previously in Section 5.1, the GRI reaction scheme is being used outside its optimised range (i.e. the pressure exceeds the validated range), and in this section the impact will be investigated. For the validation of its use the results from CHEMKIN are compared with the results obtained by the Bougrine flame speed correlation, shown in Figure 28. Bougrine verified his relation by using the same reaction scheme, but he compared it with other reaction kinetic schemes and established that the GRI mechanism is valid for higher pressures [13].

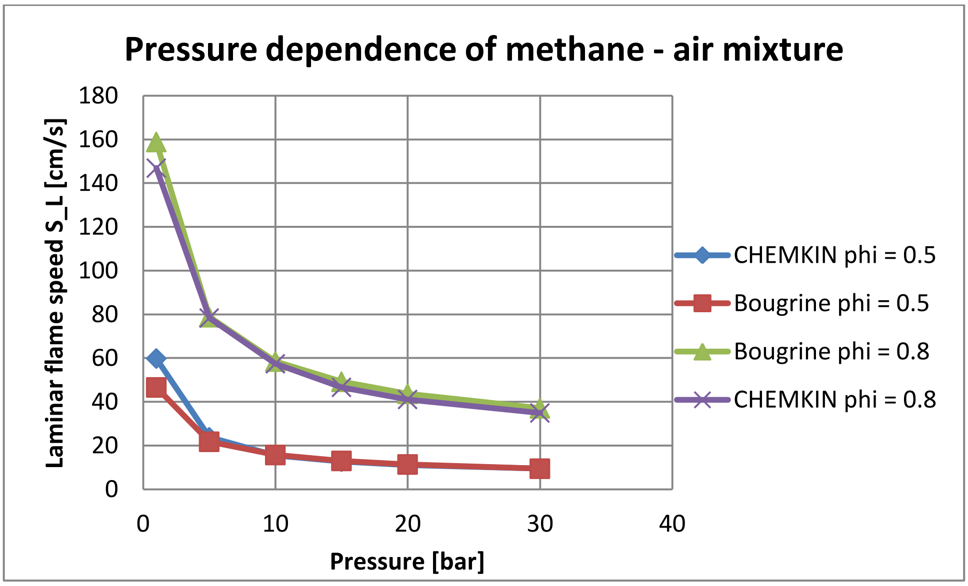

Figure 28 Pressure dependence of the laminar flame speed

The results show the same trend and absolute values when the pressure increases. The results for the equivalence ratio of 0.5 are outside the Bougrine limits, but it is believed that the scaling for methane mixtures works fine and the problems are caused by the hydrogen scaling, implying that it can be used in this verification. Because the results are very similar it is expected that the use of the GRI 3.0 reaction mechanism is unlikely to cause any problems.

6.1.2 General output

The results shown here give an impression of the program's capabilities, i.e. how the presence of the various components in the gas change, as they are created and/or used by the reactions that are going on, and how the main flow parameters change. These results are shown in Figure 29 and Figure 30. When the general flow properties are considered it is clear where the flame is located as this causes a change in the density, velocity and temperature. The density needs more time to settle in comparison with the temperature and velocity, because some reactions need more time to complete.

The typical residence time for a gas turbine combustor is 10-20ms. The residence time shown in the figure below is at about 11 ms, corresponding to a spatial position of 0.25 cm. At this point all major species except the NO_x are at their final value. The NO_x keeps on increasing with an increasing residence time in the presence of hot gas; this indicates the importance of choosing the correct residence time.

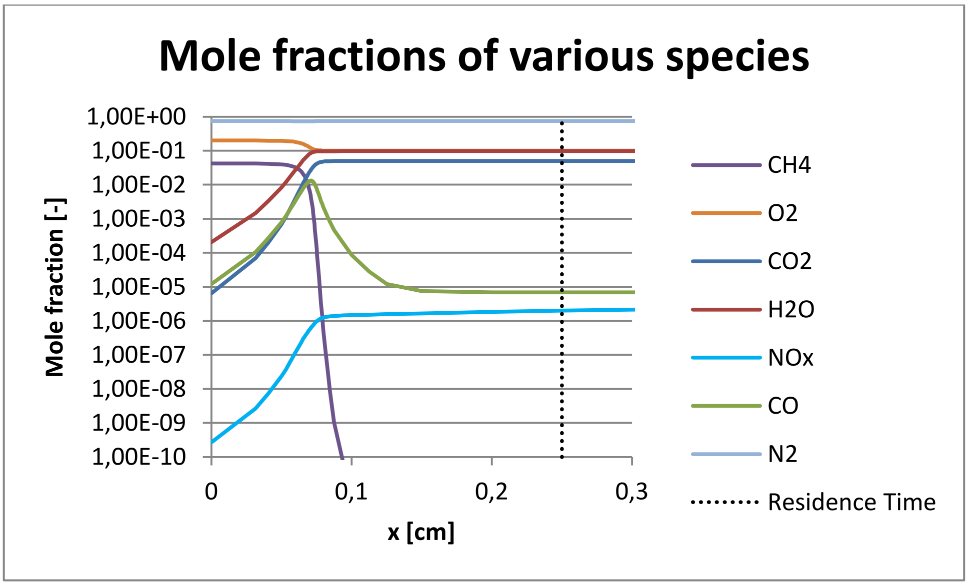

Figure 29 Change of mole fraction of the major components (ϕ=0.5, T=673K, P=15 bar, 0%vol H_2)

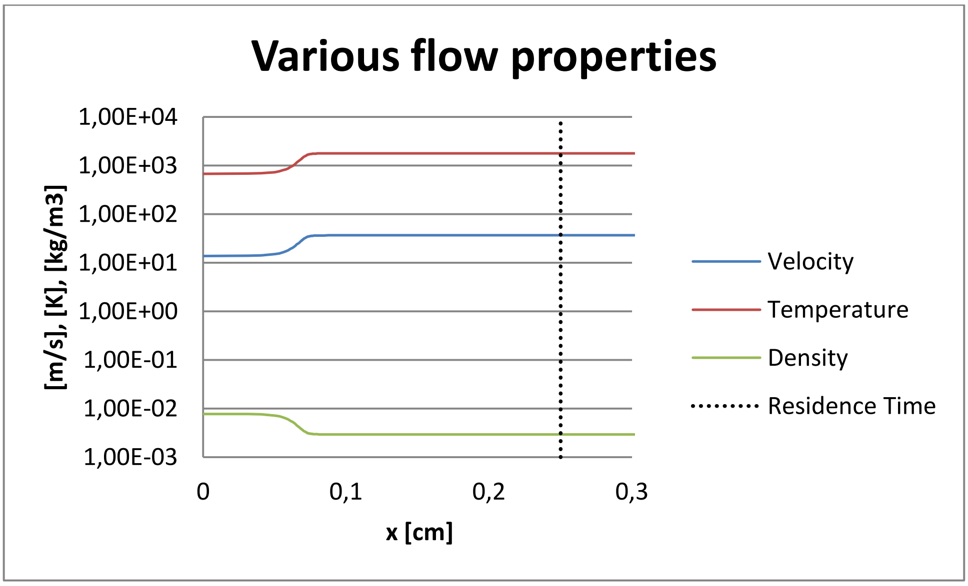

Figure 30 Change of the general flow properties (ϕ=0.5, T=673K, P=15 bar, 0%vol H_2)

6.1.3 Pressure dependence of the laminar flame speed

This section shows how the laminar flame speed changes when the pressure and hydrogen content changes. The calculations are performed with CHEMKIN at the same inlet temperature and equivalence ratio, 673K and 0.5 respectively. Leaving the pressure and hydrogen addition variable, the pressure varied from 1 to 30 bar and the hydrogen addition varied from 0 to 20%vol. The results are shown in Figure 31 below.

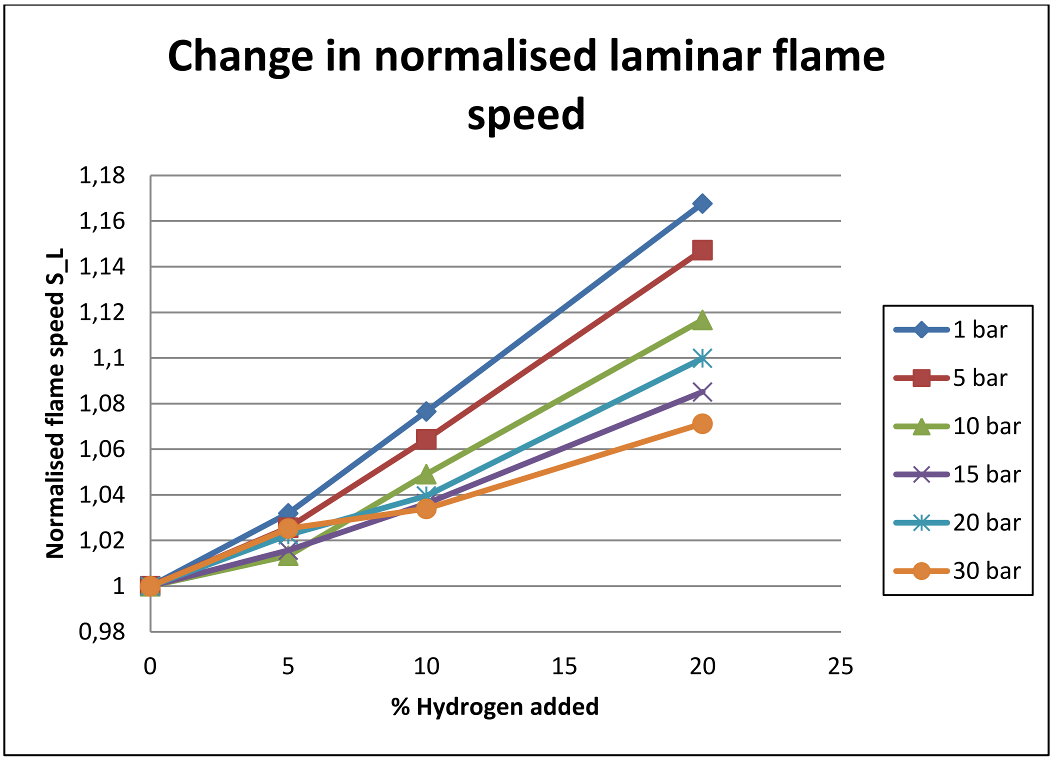

Figure 31 Calculated pressure dependence of the laminar flame speed

The results show the same behaviour as the results in the laminar flame speed section earlier; the increase of the flame speed with hydrogen addition decreases with an increasing pressure. This can be seen by the decrease of the slope of the lines in the above figure.

The change in the slope can be described with a power law type relation. When a linear fit is applied to each of the curves in Figure 31 a power law (41) can be used to describe the pressure effect on the slope, the intersection of the y-axis is the same for all equations (42). Thus a basic relation can be created to estimate the impact of hydrogen addition at a certain pressure (43). There is no temperature effect included in this analysis.

$$y = a \cdot x^{n} \tag{41}$$

$$slope \ = 0.00906 \cdot \ (P/P_o)^{-0.24542} \, , with \ P_0 = 1 \ bar \tag{42}$$

$$\frac{S_L\ (P, \alpha\ \%H_2)}{S_L(P, 0\%H_2)} = 0.00906 \cdot \left(\frac{P}{P_0}\right)^{-0.24542} \cdot \alpha + 1 \tag{43}$$

6.1.4 Laminar flame speeds

As mentioned before the simulations are split into three different groups depending on the conditions; Table 9 serves as a recapitulation of these groups. With these simulations a database was created that contains the laminar flame speeds. The results for methane and natural gas are plotted in the same figures for comparison. The results are shown in Figure 32 to

Figure 35.

Power Station	Connah's Quay	Cottam Development Centre	Enfield
GT type	General Electric 9FA	Siemens SGT5-4000F	Alstom GT26
Pressure	15 bar	20 bar	30 bar
Temperature	400 ^{o}C	460 ^{o}C	550 ^{o}C
Set number	Set 1	Set 2	Set 3

Table 9 Defining the three sets for the simulations

The PREMIX program is also capable of solving the multi-component transport equations instead of the mixture-averaged transport equations. When this is done the computational time increases dramatically from a few minutes to about an hour. The difference in flame speed is about a few percent, so it indicates that the normal simulations give satisfactory results. This has been verified for $\phi = 0.35$ and for 0, 5 and 10% hydrogen addition, see Table 10 for the results. This is in accordance with the observations made by Brower [16].

Set 6, $\phi = 0.35$	0 %vol H_2	5 %vol H_2	10 %vol H_2
$S_{L,\ averaged}$ [m/s]	0.088	0.089	0.089
$S_{L,\ multicomponent}$ [m/s]	0.090	0.091	0.090
% Difference	2.14	2.26	1.70

Table 10 Effect of transport equations on laminar flame speed

All the results show the same trend, there is an increase in laminar flame speed when hydrogen is added to the fuel mixture. However the magnitude is a little smaller than one might expect; the maximum increase is about 8% at 20%vol hydrogen addition. This small increase is in accordance with the results that are shown previously in the laminar flame speed section. The results for methane and natural gas are very similar as expected, because methane is the main component of natural gas. Natural gas has a slightly higher laminar flame speed because of the presence of higher hydrocarbons.

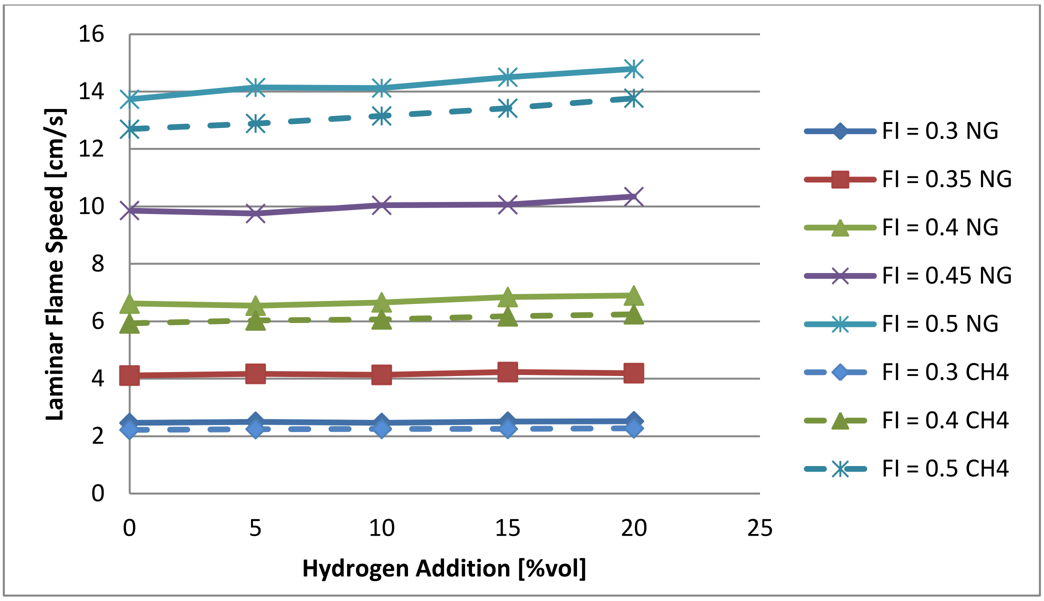

Figure 32 Effect of hydrogen on the laminar flame speed results of set 1(P = 15 bar, T = 673K)

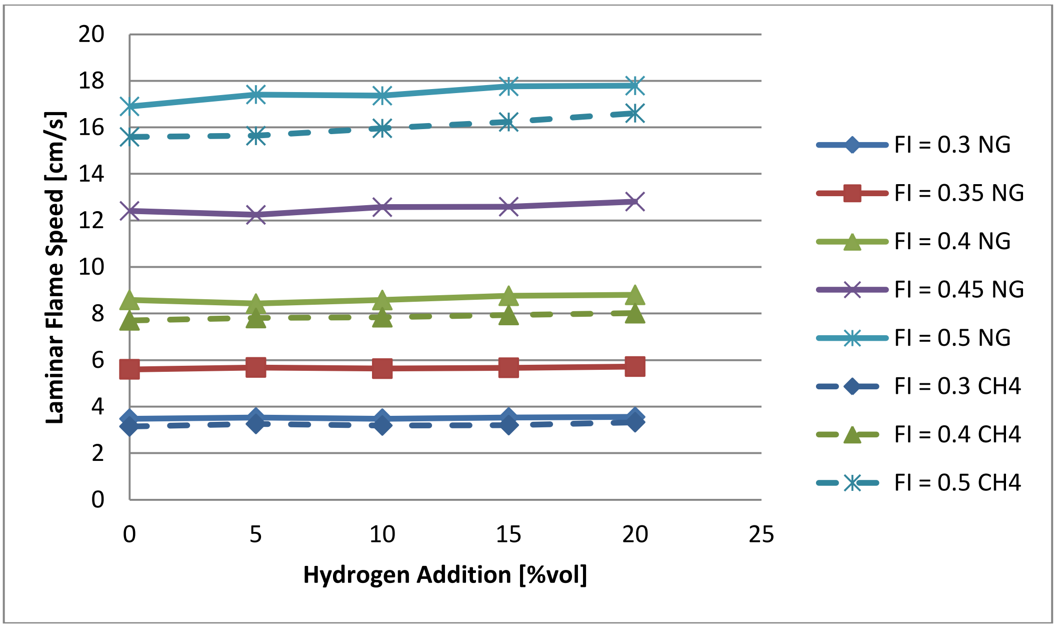

Figure 33 Effect of hydrogen on the laminar flame speed results of set 2 (P=20 bar, T = 733K)

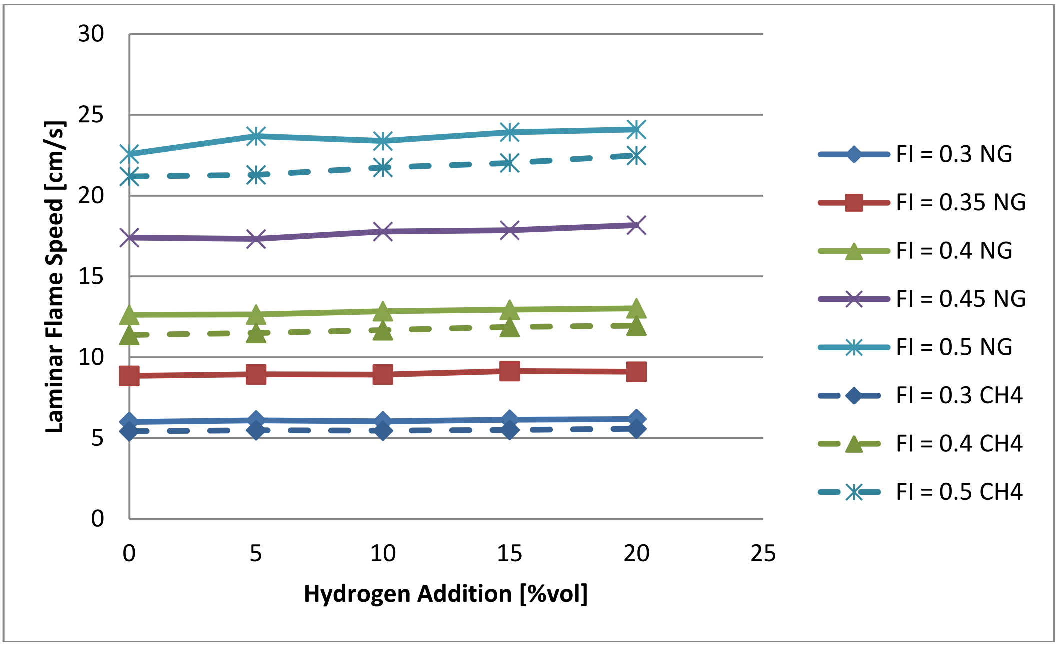

Figure 34 Effect of hydrogen on the laminar flame speed results of set 3(P = 30 bar, T = 823K)

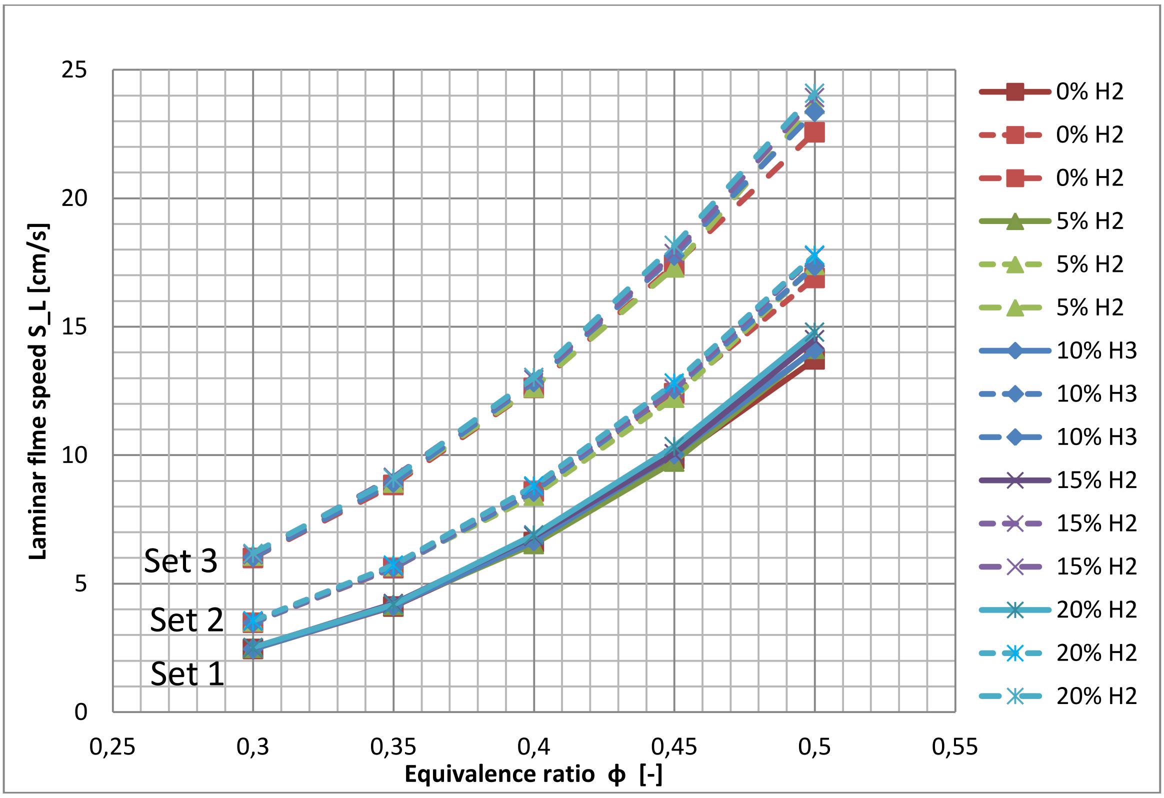

Figure 35 Impact of the equivalence ratio on the laminar flame speed for all three sets

6.1.5 Emissions results

The species profiles calculated with CHEMKIN are used for investigating the impact of hydrogen on the emissions of NO_x and CO. Of particular interest is the reproducibility of the fact that hydrogen does not affect the level of NO_x emissions and that there is no stimulation of any of the chemical reactions involved with the NO_x production.

The results from the simulations are shown in Figure 36; the error bars indicate the change of a point when 20%vol hydrogen is added. The emissions that are shown are taken at a residence time of 10-20 ms, which is typical for gas turbines, allowing a small spread in residence times. The spread in the NO_x results is small, maximum 1 ppm, that it supports the independence of the NO_x mechanisms on hydrogen content.

The CO shows more or less the expected trend, however at higher equivalence ratios, the CO starts to increase again as the equivalence ratio and thus the flame temperature increases. The steep increase at low equivalence ratios is clearly predicted, thereby creating the operating window shown earlier.

Another way to look at the emissions is to plot them versus the temperature and see if the expected increase at about 1850K happens. These scaled results are shown in Figure 37. The results have been scaled to the same pressure (15 bar). The scaling was applied using the correlation given in equation (44); a typical value for n is 0.5 [39].

$$NOx_2 = NOx_1 \left(\frac{P_2}{P_1}\right)^n \tag{44}$$

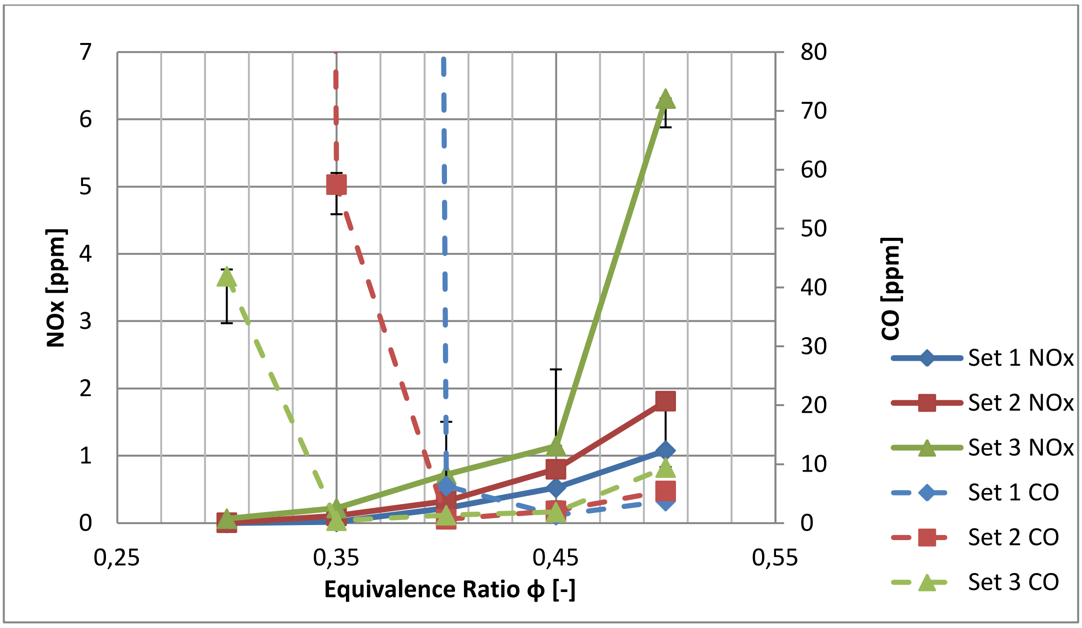

Figure 36 Emissions of each of the parameter sets

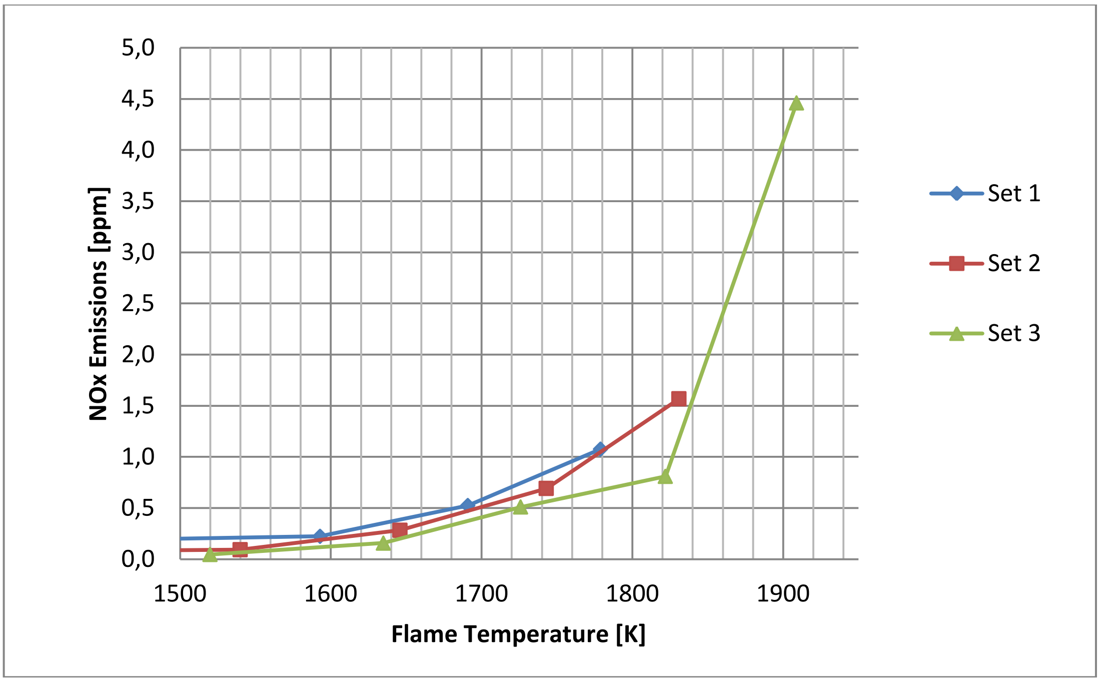

Figure 37 NO_x (pressure scaled to 15 bar)

The lines more or less collapse together onto one line which tends to validate the correlation used. This line shows the expected sharp increase in NO_x at around 1850K and tends towards zero at low temperatures.

6.1.6 Characteristic burning time

Based on the output from PREMIX the characteristic burning time has been calculated. The results of these calculations are presented in this section. Table 11 shows results for the maximum gradient method and Table 12 shows results for the 10-90% temperature method.

The results of both methods for 5%vol hydrogen addition are shown in Figure 38. Both methods show the same trend, the time needed for the temperature rise decreases with an increase in equivalence ratio. The numbers in the tables indicate that the burning time decreases slightly when hydrogen is added; as expected basis of the increased reactivity. The typical burning time of a gas turbine is 3-4 ms; the corresponding equivalence ratios are at the expected value.

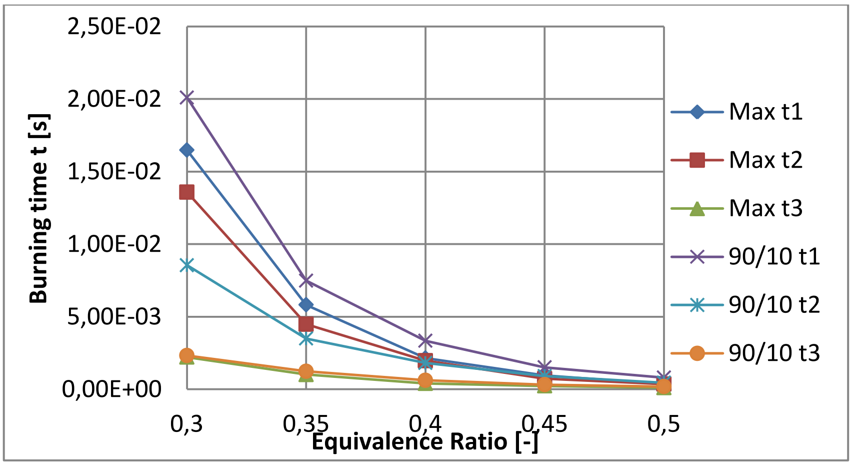

Figure 38 Characteristic burning time (5%vol hydrogen) for Set 1, 2 & 3 conditions

Set 1, 15 bar, 400 C	ϕ = 0.3	ϕ = 0.35	ϕ = 0.4	ϕ = 0.45	ϕ = 0.5
0% H2	1.68E-02	5.95E-03	2.03E-03		3.89E-04
5%H2	1.65E-02	5.83E-03	2.15E-03	9.62E-04	3.56E-04
10% H2	1.62E-02	5.90E-03	2.01E-03	9.05E-04	3.70E-04
15%H2	1.58E-02	5.51E-03	1.91E-03	9.26E-04	3.53E-04
20% H2	1.57E-02	5.79E-03	1.89E-03	8.61E-04	3.95E-04
Set 2, 20 bar, 460 C	ϕ = 0.3	ϕ = 0.35	ϕ = 0.4	ϕ = 0.45	ϕ = 0.5
0% H2	1.42E-02	4.58E-03	1.76E-03	6.66E-04	3.63E-04
5%H2	1.36E-02	4.48E-03	1.97E-03	7.30E-04	3.62E-04
10% H2	1.42E-02	4.56E-03	1.86E-03	6.74E-04	3.65E-04
15%H2	1.36E-02	4.40E-03	1.80E-03	6.74E-04	3.42E-04
20% H2	1.35E-02	4.26E-03	1.74E-03	6.54E-04	5.86E-04
Set 3, 30 bar, 550 C	ϕ = 0.3	ϕ = 0.35	ϕ = 0.4	ϕ = 0.45	ϕ = 0.5
0% H2	2.27E-03	1.09E-03	4.03E-04	2.34E-04	1.23E-04
5%H2	2.22E-03	1.01E-03	4.05E-04	2.40E-04	1.12E-04
10% H2	2.25E-03	1.07E-03	3.83E-04	2.27E-04	8.28E-05
15%H2	2.24E-03	1.05E-03	3.91E-04	2.29E-04	1.12E-04
20% H2	2.13E-03	1.08E-03	3.87E-04	2.19E-04	8.12E-05

Table 11 Characteristic times [s] of the Maximum gradient method

Set 1, 15 bar, 400 C	**ϕ = 0.3**	**ϕ = 0.35**	**ϕ = 0.4**	**ϕ = 0.45**	**ϕ = 0.5**
0% H2	2.08E-02	7.71E-03	3.28E-03		8.54E-04
5%H2	2.01E-02	7.48E-03	3.35E-03	1.52E-03	8.11E-04
10% H2	2.08E-02	7.64E-03	3.24E-03	1.43E-03	8.15E-04
15%H2	2.01E-02	7.28E-03	3.08E-03	1.43E-03	7.82E-04
20% H2	1.99E-02	7.43E-03	3.05E-03	1.35E-03	7.12E-04
Set 2, 20 bar, 460 C	**ϕ = 0.3**	**ϕ = 0.35**	**ϕ = 0.4**	**ϕ = 0.45**	**ϕ = 0.5**
0% H2	8.79E-03	3.56E-03	1.72E-03	8.65E-04	4.67E-04
5%H2	8.55E-03	3.50E-03	1.82E-03	9.07E-04	4.59E-04
10% H2	8.79E-03	3.54E-03	1.76E-03	8.66E-04	4.63E-04
15%H2	8.54E-03	3.44E-03	1.69E-03	8.65E-04	4.45E-04
20% H2	8.47E-03	3.48E-03	1.68E-03	8.36E-04	7.12E-04
Set 3, 30 bar, 550 C	**ϕ = 0.3**	**ϕ = 0.35**	**ϕ = 0.4**	**ϕ = 0.45**	**ϕ = 0.5**
0% H2	2.40E-03	1.22E-03	5.92E-04	3.19E-04	2.16E-04
5%H2	2.33E-03	1.24E-03	6.22E-04	3.23E-04	1.93E-04
10% H2	2.37E-03	1.21E-03	6.03E-04	3.09E-04	2.08E-04
15%H2	2.26E-03	1.15E-03	5.76E-04	3.08E-04	1.89E-04
20% H2	2.22E-03	1.17E-03	5.70E-04	2.98E-04	1.81E-04

Table 12 characteristic times [s] of the 10-90% temperature method

6.2 Turbulent flame speed

The predictions made by the three selected turbulent flame speed correlations are shown in this section. The results are grouped by correlation making it easy to investigate the impact of the different conditions on each correlation. The results are presented in Figure 39, Figure 40 and Figure 41 and the turbulent flow properties used for all three calculations in Table 13.

parameter	value
Mean flow velocity (U)	35 m/s
Velocity fluctuations (u')	10% of U
Turbulent length scale	1.18 mm

Table 13 Turbulent flow properties

The sensitivity analysis showed that these correlations are fairly robust with regards to uncertainties in the estimations of the flow and flame properties. The laminar flame speeds, which had the biggest impact on the correlations, are obtained from the CHEMKIN calculations and therefore should be predicted with reasonable accuracy. The flow properties applied should be fairly good as well, because they are based on data found in literature [25]. Therefore the results from the correlations should be reasonable.

As these are the best three correlations they produce similar turbulent flame speeds, but there is still a spread in the predicted flame speeds, just as in Figure 15. All models capture the trend of an increase in turbulent flame speed when the equivalence ratio increases.

But all three models show a different prediction of the impact of hydrogen on the turbulent flame speed. The L&C 2 correlation shows that there is only a small change in the turbulent flame speed or a decrease depending on the conditions. The L&C 3 correlation shows that hydrogen lowers the turbulent flame speed. The Brower correlation indicates that the turbulent flame speed increases when hydrogen is added.

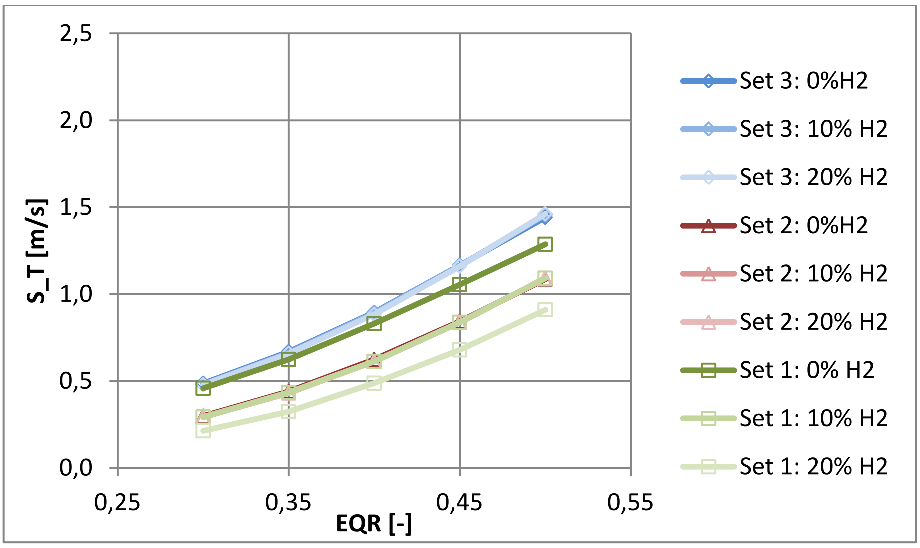

Figure 39 L&C 2 Turbulent flame speeds

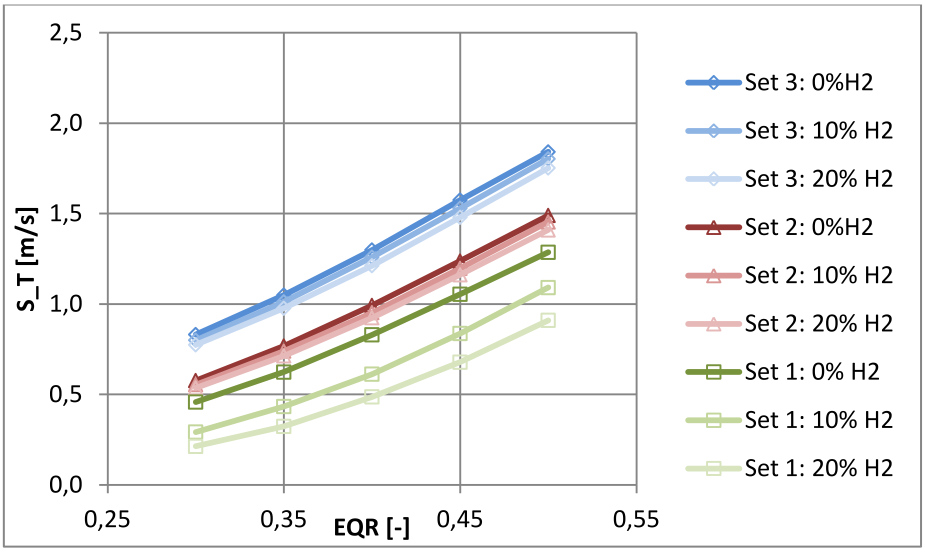

Figure 40 L&C 3 Turbulent flame speeds

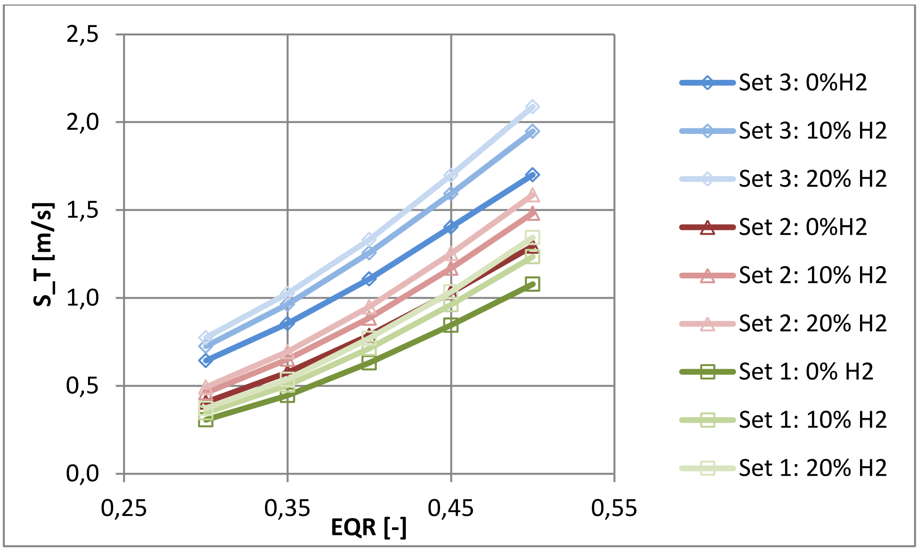

Figure 41 Brower Turbulent flame speeds

6.3 Expansion ratio calculations

The results of the calculations of expansion ratio are shown in this section. The calculations are only performed at conditions representing the Alstom GT26B gas turbine, because the results should give a good indication of the changes that will occur. The results are shown in Figure 42. When hydrogen is added the expansion ratio decreases slightly, this is indicated by the error bars. The maximum change was about 1% at 20%vol hydrogen addition.

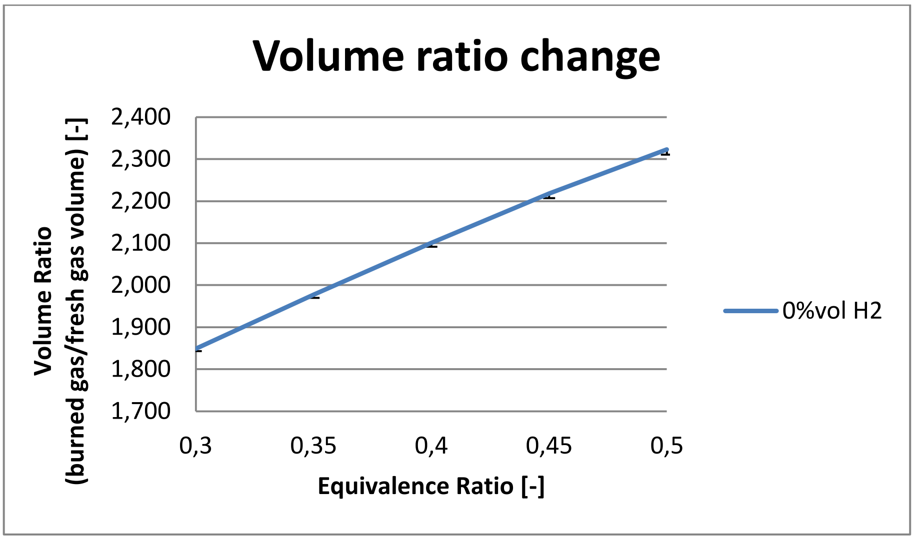

Figure 42 Expansion ratio change (error bars at 20%vol hydrogen)

6.4 Konle model results

The addition of hydrogen to natural gas leads to an increase in the laminar flame speed at the same equivalence ratio and in combination with equation (38) an increase of the flashback zone is expected, because the mean flow velocity has to increase. This is shown in Figure 43 by the movement to the right of the lines when hydrogen is added.

The operating points of the two GT26 variants are indicated by the circle and diamond in Figure 43. The lines are close to each other because the increase in laminar flame speed due to hydrogen addition is low.

On the basis of the known flashback risk for the Alstom GT26A/B gas turbine the flashback limiting curve can be created, this is shown in Figure 43 as the 0% hydrogen line. The region to the right of it is the stable region and the region to the left of it is the flashback region. When it is compared to the GT26B gas turbine, it can be seen that the latter has a higher mean flow velocity, indicating an improved flashback resistance.

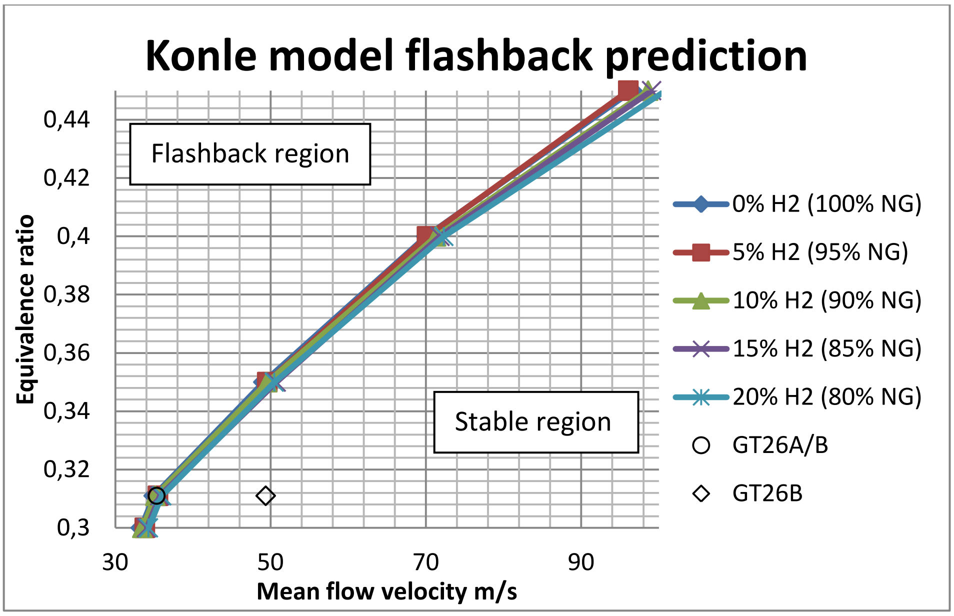

Figure 43 Konle flashback prediction

It is assumed that both machines show flashback in the same way, thus the amount of hydrogen can be increased until the limit line intersects the operating point of the B-type machine to get an estimation of how much hydrogen can be added. The laminar flame speed shows only a small increase therefore causing only a small displacement of the lines. Due to the small displacement of the lines this is not an effective method to estimate the flashback risk, because it probably overestimates the amount of hydrogen that can be added safely.

A similar exercise can be performed for a Siemens SGT-700 gas turbine, due to the small increase in laminar flame speed the results are similar to the results shown above and therefore they are not shown.

The flashback assessment focused on the likelihood of flashback at normal operating conditions, where the equivalence ratio is relatively low. It may be possible that the likelihood of flashback is greater during start up or shut down, when operating conditions are considerably different (see Appendix III).

7 Discussion of results

In this section the results from the simulations that are shown in the previous section will be thoroughly analysed to estimate the impact of hydrogen addition on E.ON's GT's. The four main subjects of flame speeds, emissions, combustion dynamics and flashback, are analysed separately for their sensitivity to hydrogen.

7.1 Flame speeds

The laminar flame speed does not increase dramatically when hydrogen is added to the natural gas; the maximum increase is under 10% at 20%vol hydrogen addition. The results tend to show a linear increase in the laminar flame speed matching the behaviour based on the literature study. The three sets of laminar flame speed correlations show similar results, namely a linear increase in flame speed when hydrogen is added and this increase grows when the equivalence ratio is increased. However there was no information found in literature to validate the results; the above mentioned arguments make the results look reasonable.

The predictions of the effects of hydrogen addition on the turbulent flame speed show different results; the turbulent flame speed can change in all directions. The results from literature indicate that hydrogen enhances the turbulent flame speed [28]. Due to the lack of information at gas turbine conditions the calculations could not be verified, so the quality of the predictions is uncertain. The Brower correlation seems to be a promising correlation to predict the turbulent flame speed, but this may change when additional information becomes available.

The Brower correlation predicts a maximum increase in the turbulent flame speed of 25% when 20%vol hydrogen is added. The typical increase at 20%vol hydrogen is about 22%, this increase is the same for all three GT types. These results show that the turbulent flame speed is more sensitive to hydrogen addition than the laminar flame speed.

7.2 Emissions

The results from the literature indicated that the amount of CO could be reduced by adding hydrogen, one of the reasons is the decreasing blow-off limit. This shift in CO concentration can be seen very weakly in the results from PREMIX, but it is not unambiguous enough to presume it is actually happening. The CO emissions are not affected or slightly favoured when hydrogen is added.

The NO_x emissions show the same trend as was expected on basis of the literature research. There is a sharp increase in the NO_x at temperatures greater than 1800-1850K and hydrogen barely affects the level of NO_x emissions.

A method developed by Hornsby and Norster, sometimes used to estimate the NO_x emissions, is based on the mixing quality of the fuel air mixture [40]. The results are typically plotted in a diagram with different curves of mixing quality, so called S-curves, starting at perfectly mixed(S=0) and then gradually decreasing the mixing quality (S>0).

In Figure 44 the CHEMKIN results are compared to the mixing quality model predictions. The CHEMKIN results are plotted in two ways. The red line shows the results from the simulations of set 1. The black line shows the exponential fit created from scaling and combining the results from all three sets of data with the aid of equation (44). The CHEMKIN results are close to the perfectly mixed line, indicating that the results are in the right order.

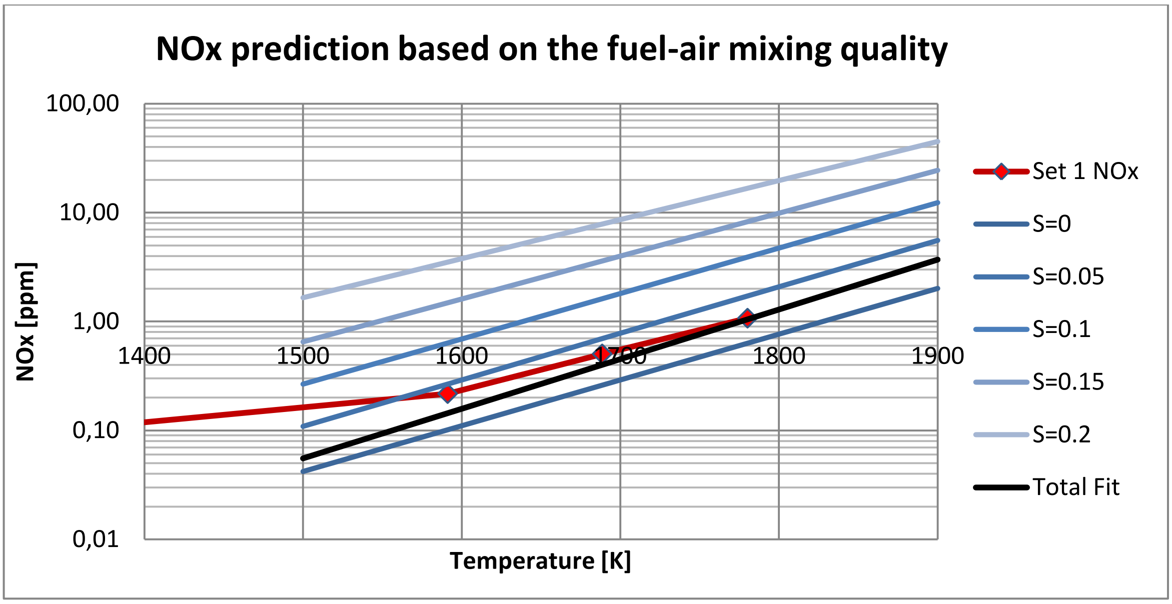

Figure 44 Comparison of the CHEMKIN results with the mixing quality/S-curves model

7.3 Combustion Dynamics

As mentioned before was there no major change in the laminar flame speed when hydrogen was added, thus based on the source term analysis the combustion dynamics will not change a lot. Also the effect depends on the formulation of the source term and the power of the laminar flame speed term in the source term.

The other method was by calculating the impact on the flame transfer function. The phase, thus the burning time, decreases slightly when hydrogen is added to the fuel, typically this change is not more than 5%. The amplification, the expansion ratio, hardly changes; when hydrogen is added to the fuel it decreases by less than 1%. The change is so small due to the excessive amounts of air that are present at lean combustion conditions.

Both methods show that there will be a small change in the factors that drive the combustion dynamics. These changes are so small that it is unlikely that the combustion dynamics will change dramatically; small changes in the dynamics can generally be compensated for during tuning of the gas turbine.

7.4 Flashback

The results of the Konle model are strongly dependent on the change of the laminar flame speed, this can be seen in equation (38). Due to the strong dependence on the laminar flame speed in combination with the minor change of the laminar flame speed when hydrogen is added, the results from the Konle model indicate that high levels of hydrogen addition may be allowed. Since there is no relevant literature data available for comparison it is hard to establish whether the predictions are correct or overestimated.

8 Conclusions and recommendations

During the study much information was obtained about the impact of hydrogen addition, but there were also some significant gaps identified. Here the conclusions and recommendations are presented of the study on the effects of hydrogen addition to natural gas and the impact on gas turbine combustors.

8.1 Conclusions

The current UK regulations do not allow any hydrogen in the gas grid, and this has to change before any hydrogen can be added to it. The specifications set by the gas turbine manufacturers are type and model dependent, but at the moment maximum 5%vol hydrogen can be burned. These limitations may be changed if experiments show that it is possible to burn higher levels of hydrogen safely.

Interchangeability methods

The classic Weaver, AGA and Dutton interchangeability methods are not suited for the prediction of the impact hydrogen addition to natural gas for gas turbine operation. More advanced methods are needed to predict the impact on gas turbines. The classic methods would predict that 15-25vol% of hydrogen could be added without significant problems, but as mentioned above these values cannot be relied upon due to the limitations of these methods.

Flame speeds

At the low equivalence ratios encountered in gas turbines the laminar flame speed increases by a maximum of 10% at 20%vol hydrogen addition. This increase is the largest at conditions representing the Alstom gas turbine, and the effects are lower at Siemens and G.E. gas turbine conditions.

The sensitivity analysis showed that the chosen turbulent flame speed correlations are the most sensitive to uncertainties in the laminar flame speed and not the turbulent flow properties. The prediction of the turbulent flame speed strongly depends on the chosen correlation and the Brower correlation seems to be the most promising one.

Based on the Brower equation there is maximum of 25% increase in turbulent flame speed when 20%vol hydrogen is added to natural gas; the typical increase is about 20% at 20%vol hydrogen addition and is the same for all three types of GT's, making the turbulent flame speed more sensitive to hydrogen than the laminar flame speed.

Emissions

Instead of causing problems, hydrogen addition tends to favour the emissions. The NO_x remains substantially the same when hydrogen is added to the fuel, while maintaining the same combustion temperature. The CO could be lowered by hydrogen addition, due to the extension of the lean blow off limit, this was seen clearly in experimental results [28] , but is not as clearly demonstrated by the analytical results in Figure 36.

Combustion Dynamics

The impact on the combustion dynamics was determined in two ways. The first method looked at the source term of the turbulent combustion. Due to the dependence on the laminar flame speed it does not change much. This analysis indicates that if there are problems due to the change in laminar flame speed it is the likeliest that they will occur in the mixtures that are the fuel richest.

The second method looked at the change in the flame transfer function. The amplification by the flame changed marginally when hydrogen was added. The phase component showed a larger change typically about 5%. By combining both results it is unlikely that the flame transfer function will change significantly due to hydrogen addition.

Flashback

The results from the Konle model indicate that there will not be a great change in CIVB flashback risk for the Alstom GT 26 under typical operating conditions when hydrogen is added, because there is only a small change in the laminar flame speed. The risk of WBL flashback is not assessed because the current method is unsuited. Since the combustion dynamics did not change much it is unlikely that flashback due to combustion instabilities will be a problem when hydrogen is added.

Overall

Different methods have been used to predict the impact of the increased reactivity of the fuel mixture due to hydrogen enrichment on the combustion in gas turbines. These methods indicate that the hydrogen enrichment of natural gas probably will not cause major problems in the selected gas turbines. The only concern is about the change in turbulent flame speed of 22% at 20%vol hydrogen, because it is a reasonably large increase and the prediction contains significant uncertainties. The latter indicates the main concern, namely the lack of information on hydrogen in natural gas at gas turbine conditions. The results suggest that low levels of hydrogen are unlikely to cause problems, but it is impossible to define a maximum hydrogen limit. Ideally some experiments under representative conditions should be performed to allow a more robust assessment.

8.2 Recommendations

In this report a number of calculations have been executed to estimate the impact of hydrogen addition to natural gas on gas turbine performance. Where possible, the results have been compared with results from literature, however there was not a lot of information found at gas turbine relevant conditions. Therefore it was impossible to compare all the results with literature results. It would be valuable to track newly published research and engage in relevant research projects. It would also be useful to execute a series of experiments at relevant conditions to get a better understanding of the impact on combustion and an indication of the validity of the results that could not be verified.

As there is a possibility that experiments will be conducted at the Gas Turbine Research Centre at the University of Cardiff, a test program to address the issues has been developed and is given in Appendix II. This program should give a better understanding about the effects of hydrogen addition at high pressure and gas turbine flow conditions. In these experiments the flashback risk, emissions, combustion dynamics and flame shape could be investigated.

The calculations in this report have been performed at conditions that are very similar to the base load operating conditions of a gas turbine. The effect of hydrogen addition during start up, i.e. from ignition to base load, was not investigated. As the conditions during start up differ from the base load conditions, as is shown in the analysis in Appendix III, it is recommended that the effects of hydrogen enrichment on start up are reviewed.

References

[1] Gas Safety (Management) Regulations 1996

[2] BP and the International Gas Union, “Guidebook to Gas Interchangeability and Gas Quality”.

[3] Abbott D, “Practical examples of the impact of variations in gas composition on gas turbine operation and performance”, presentation Gas to Power Europe Forum, January 2012.

[4] EASEE-Gas, Common Business Practice, Number: 2005-001/0, Harmonisastion of Natural Gas Quality, February 2005

[5] International Institution of Gas Engineers & Managers,”Application of Natural Gas and fuel oil systems to gas turbines and supplementary and auxiliary fired burners”, Utilization Procedures, IGE/UP/9 Edition 2, communication 1705, 2004.

[6] Weaver R., “Formulas and Graphs for representing the interchangeability of Fuel Gases”, Journal of Research of the National Bureaus of Standards, Vol. 46, No 3, March 1951 Research paper 2193

[7] Ennis C.J., Botros K.K. and Engler D., “On the Difference between US Example Gases, European Limit Gases, and their Respective Interchangeability Indices”, AGA – Operations Conference & Biennial Exhibition, Pittsburgh Pa, May 2009.

[8] Steinmetz, G.F., The evolutionary path towards compatible requirements between gas appliance performance and natural gas quality, Gas quality and measurement 1989, conference proceedings, institute of gas technology 1989

[9] Dutton B.C., “A new dimension in gas interchangeability”, Communication 1246, 50th Autumn meeting at Eastbourne, Institution of Gas Engineers, 1984.

[10] Di Sarli V., Di Benedetto A., “Laminar burning velocity of hydrogen-methane/air premixed flames”, International Journal of Hydrogen Energy 32 (2007) 637-646

[11] Yu G., Law C.K. and WU C.K., “Laminar Flame Speeds of Hydrocarbon + Air Mixtures with Hydrogen Addition”, Combustion and Flame 63: 339-347 (1986)

[12] Shelil N. et al, “Premixed Swirl Combustion and Flashback Analysis with Hydrogen/Methane Mixtures”, 48th AIAA meeting, AIAA paper 2010-1169

[13] Bougrine S., Richard S., Nicolle A. and Veynante D., “Numerical study of laminar flame properties of diluted methane-hydrogen-air flames at high pressure and temperature using detailed chemistry”, International Journal of hydrogen energy 36 (2011) 12035-12047.

[14] Halter F., Chauveau C., Djebaïli-Chaumeix N., Gökalp I., “Characterization of the effects of pressure and hydrogen concentration on laminar burning velocities of methane-hydrogen-air mixtures”, Proceedings of the Combustion Institute 30 (2005) 201-208

[15] Not Used

[16] Brower M., Petersen E. et al, “Ignition delay time and laminar flame speed calculations for natural gas/hydrogen blends at elevated pressures”, ASME paper GT2012-69310.

[17] Panne T. et al, “Evaluation of Combustor Concepts for H_2-Combustion”, DLR Institute of Combustion Technology, Final Report of a study performed by DLR for E.ON, 08-02-2011.

[18] Lipatnikov A., “Fundamentals of Premixed Turbulent Combustion”, CRC Press, Taylor and Francis Group, 2013.

[19] Lefebvre A.H. and Ballal D.R., “Gas turbine combustion, alternative fuels and emissions”,3th edition, CRC Press, Taylor and Francis Group, 2010.

[20] Venkateswaran P., Marshall A.D. et al, “Global turbulent consumption speeds ($S_{T,GC}$) of H_2”ASME GT 2009 59685.

[21] Wang Q. McDonell V. et al, “Correlating flashback tendencies for premixed injection of hydrogen and methane mixtures at elevated temperature and pressure“, ASME GT 2009 59500.

[22] Daniele S. and Jansohn P., “Correlations for turbulent flame speed of different syngas mixtures at high pressure and temperature”, ASME paper GT 2012 69611.

[23] McBridge B.J., Gordon S. and Reno M.A., “Coefficients for Calculating Thermodynamic and Transport Properties of Individual Species”, NASA Technical Memorandum 4513, October 1993

[24] Perry R.H. and Green D.W., “Perry’s Chemical Engineers Handbook”, 7th edition, McGraw-Hill, 1997.

[25] Griebel P., Bomback R., Inauen A. et al, “Flame characteristics and turbulent flame speeds of turbulent, high-pressure, lean premixed methane/air flames“, ASME GT 2005-68565.

[26] Poinsot T. and Veynante D., “Theoretical and Numerical Combustion”, 3th edition

[27] Lieuwen T., McDonell V., PetersenE. And Santavicca D., “Fuel flexibility influences on premixed combustor blowout, flashback, autoignition and stability“, Journal of Engineering for Gas Turbines and Power, January 2008 vol. 130.

[28] Griebel, P., Boschek E. and Jansohn P., “Lean blowout limits and NO_X Emissions of turbulent, lean Premixed, hydrogen-enriched methane/air flames at high pressure”, ASME paper GT2006-90490

[29] Morris, J.D. Symonds, R.A. et al., “Combustion aspects of application of hydrogen and natural gas fuel mixtures to MS9001E DLN-1 gas turbines at Elsta plant, Terneuzen, the Netherlands”, ASME paper 98-GT-359

[30] Abbott D.J., Bowers J.P. and James S.R., “The impact of natural gas composition variations on the operation of gas turbines for power generation”, 5th international conference on The Future of Gas Turbine Technology, 17-18 October 2012 Brussels, Belgium.

[31] Tuncer O., Acharya S. and Ho Uhm J., “Dynamics, NO_X and flashback characteristics of confined pre-mixed hydrogen enriched methane flames”, ASME paper GT2007-28158.

[32] Kok, J, “Combustion Dynamics and the effect of Gas Composition”, University of Twente, published on the Dutch Gas Turbine Association’s website, http://www.dgta.nl/about-dgta/projects/changing-gas-composition, downloaded 13/08/09.

[33] Abbott D.J., “The prediction of acoustic feedback driven oscillations in gas turbine combustors”, Hand outs of the two day seminar Turbulent Combustion of Gases and Liquids organised by IMechE, December 1998

[34] Fritz J., Kröner M. And Sattelmayer T., “Flashback in a swirl burner with cylindrical premixing zone“, ASME paper GT 2001-GT-0054

[35] Fritz J., Kröner M. And Sattelmayer T., “Flashback limits for combustion induced vortex breakdown in a swirl burner”, ASME paper GT 2002-30075

[36] PREMIX, one-dimensional steady premixed laminar flame code, CHEMKIN-II version 2.55 March 1994.

[37] Kok J.B.W., PREMIX a program for computing steady premixed laminar flames, University of Twente 2009.

[38] Mayer C., Sangl J., Sattelmayer T. et al, “Study on the operational window of a swirl stabilized syngas burner under atmospheric and high pressure conditions”, ASME paper GT 2011-45125

[39] Abbott D.J., Graham D. and Cannon M., “NO_x Performance of Gas Turbine Based Technologies: Final Report”, 3 November 2000 for the Department of Trade and Industry.

[40] Hornsby C. and Norster E.R.," Application of CFD to DLN Combustion", Int. Gas Turbine and Aeroengine Congress & Exhibition, Orlando, Florida, June 2-5, 1997, ASME 97-GT-371, 1997.

[41] Konle M. and Sattelmayer T., "Time scale model for the prediction of the onset of flame flashback driven by combustion induced vortex breakdown (CIVB)", ASME GT 2009-59606

[42] Smith G.P., Golden D.M., Frenklach M., Moriarty N.W., Eiteneer B., Goldenberg M., Bowman C.T., Hanson R.K., Song S., Gardiner Jr W.C., Lissianski V.V. and Qin Z., http://www.me.berkeley.edu/gri_mech/

[43] Johnson F., Rue D.M., "Gas Interchangeability tests, Evaluating the Range of Interchangeability of Vaporized LNG and Natural Gas", the Gas Technology Institute report GRI-03/0159 , April 2003.

Appendix I Bougrine flame speed correlation

In this appendix the detailed version of the Bougrine equation is shown, they show the values of the various constants and the methods of calculating the various sub factors.

a0	2.72E-06	αt4	-1.0359	a6	-2.25E-01	αres4	-8.69E-04
a1	2.897	f1	-1.115	αp0	-5.41E-01	f2	1.32E+00
a2	150.817	λt0	0.5	αp1	1.35E-01	λp0	-1.90E+00
a3	4.539	λt1	0.58	αp2	-1.25E-02	λp1	3.56E-02
a4	-2.448	λ0	1.4	αp3	-5.17E-04	λp2	-1.63E-04
a5	-0.0017	λ1	3.39E-07	αp4	2.29E-04	ϕ0	1.75E+00
αt0	3.2466	λ2	-1.17E-06	αres0	4.16E+00	ϕ1	-1.75E+00
αt1	-1.0709	λ3	1.17E-07	αres1	-1.74E+00	ϕ2	6.25E-01
αt2	0.1517	λ4	-3.75E-09	αres2	5.12E-01	ϕ3	-3.80E-02
αt3	-3.20E-04	λ5	1.40E-10	αres3	-4.70E-03	ϕ4	1.38E-01
P0	1.0E5	T0	300				

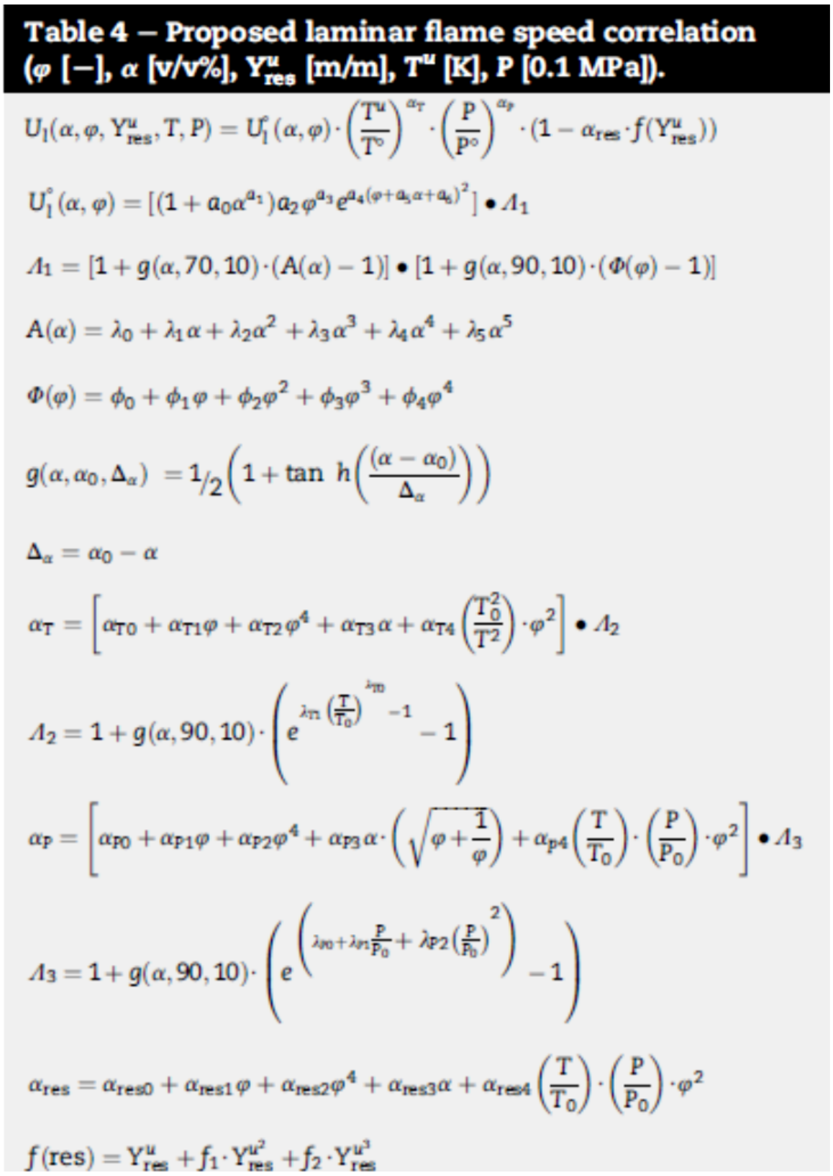

Table 4 – Proposed laminar flame speed correlation (φ [–], α [v/v%], Y^u_{res} [m/m], T^u [K], P [0.1 MPa]).

$$U_l(\alpha,\varphi,Y^u_{res},T,P) = U_l^\circ(\alpha,\varphi)\cdot\left(\frac{T^u}{T^\circ}\right)^{\alpha_T}\cdot\left(\frac{P}{P^\circ}\right)^{\alpha_P}\cdot\left(1-\alpha_{res}\cdot f(Y^u_{res})\right)$$

$$U_l^\circ(\alpha,\varphi) = \left[(1+a_0\alpha^{a_1})a_2\varphi^{a_3}e^{a_4(\varphi+a_5\alpha+a_6)^2}\right]\bullet\Lambda_1$$

$$\Lambda_1 = [1+g(\alpha,70,10)\cdot(A(\alpha)-1)]\bullet[1+g(\alpha,90,10)\cdot(\Phi(\varphi)-1)]$$

$$A(\alpha) = \lambda_0+\lambda_1\alpha+\lambda_2\alpha^2+\lambda_3\alpha^3+\lambda_4\alpha^4+\lambda_5\alpha^5$$

$$\Phi(\varphi) = \phi_0+\phi_1\varphi+\phi_2\varphi^2+\phi_3\varphi^3+\phi_4\varphi^4$$

$$g(\alpha,\alpha_0,\Delta_\alpha) = 1/2\left(1+\tan\ h\left(\frac{(\alpha-\alpha_0)}{\Delta_\alpha}\right)\right)$$

$$\Delta_\alpha = \alpha_0-\alpha$$

$$\alpha_T = \left[\alpha_{T0}+\alpha_{T1}\varphi+\alpha_{T2}\varphi^4+\alpha_{T3}\alpha+\alpha_{T4}\left(\frac{T_0^2}{T^2}\right)\cdot\varphi^2\right]\bullet\Lambda_2$$

$$\Lambda_2 = 1+g(\alpha,90,10)\cdot\left(e^{\lambda_{T1}\left(\frac{T}{T_0}\right)^{\lambda_{T0}}-1}-1\right)$$

$$\alpha_P = \left[\alpha_{P0}+\alpha_{P1}\varphi+\alpha_{P2}\varphi^4+\alpha_{P3}\alpha\cdot\left(\sqrt{\varphi+\frac{1}{\varphi}}\right)+\alpha_{p4}\left(\frac{T}{T_0}\right)\cdot\left(\frac{P}{P_0}\right)\cdot\varphi^2\right]\bullet\Lambda_3$$

$$\Lambda_3 = 1+g(\alpha,90,10)\cdot\left(e^{\left(\lambda_{P0}+\lambda_{P1}\frac{P}{P_0}+\lambda_{P2}\left(\frac{P}{P_0}\right)\right)^2}-1\right)$$

$$\alpha_{res} = \alpha_{res0}+\alpha_{res1}\varphi+\alpha_{res2}\varphi^4+\alpha_{res3}\alpha+\alpha_{res4}\left(\frac{T}{T_0}\right)\cdot\left(\frac{P}{P_0}\right)\cdot\varphi^2$$

$$f(\text{res}) = Y^u_{res}+f_1\cdot Y^{u^2}_{res}+f_2\cdot Y^{u^3}_{res}$$

Appendix II Cardiff rig testing program

High Pressure Tests

		Steady points										LBO			Flashback test	
Parameter\point		1	2	3	4	5	6	7	8	9	10	11	12	13	14	15
Pressure	[bar]	10	10	10	10	10	10	10	10	10	10	10	10	10	10	10
Temperature	[K]	673	673	673	733	673	673	673	673	673	673	673	673	673	673	673
Equivalence ratio	[-]	0.35	0.4	0.5	0.5	0.35	0.4	0.5	0.35	0.4	0.5	0.4	0.4	0.4	0.4	0.5
Hydrogen fraction fuel	[%vol]	0	0	0	0	10	10	10	20	20	20	0	10	20	10	20

Atmospheric Pressure Tests

		Steady points										LBO			Flashback test		
Parameter\point		20	21	22	23	24	25	26	27	28	29	30	31	32	33	34	35
Pressure	[bar]	1	1	1	1	1	1	1	1	1	1	1	1	1	1	1	1
Temperature	[K]	300	300	300	300	300	300	300	300	300	360	300	300	300	300	300	300
Equivalence ratio	[-]	0.35	0.35	0.35	0.4	0.4	0.4	0.5	0.5	0.5	0.5	0.35	0.35	0.35	0.35	0.4	0.5
Hydrogen fraction fuel	[%vol]	0	10	20	0	10	20	0	10	20	0	0	10	20	20	20	20

Tests 1 - 10 and 20 - 29 are performed to get an idea of the impact of hydrogen addition at various equivalence ratios.

Tests 11 - 13 and 30 - 32 are performed to investigate the lean blow out. This can be done by gradually reducing the fuel flow to the burner whilst maintaining constant air flow.

Tests 14 and 15 and 33 - 35 are performed to get an idea of the flashback risk. This can be investigated by gradually increasing the hydrogen fraction of the fuel whilst maintaining constant air flow and total heat input.

Because it is cheaper to execute tests at atmospheric pressure than at high pressure more tests are conducted at atmospheric pressure. At high pressure the basics are tested and at atmospheric pressure more variables are allowed to vary to get a good idea of the impact of hydrogen.

Appendix III Analysis of the complete GT load range

The load range investigated is shown in Figure 45 as a function of the time, covering the complete range from start up to base load of a GE 9FA.01 with DLN-2.0 combustion system. Equivalence ratios and flow velocities are based on the operation of E.ON's gas turbines at Connah's Quay Power Station and estimated using E.ON in house calculation methods. During the start up the gas turbine runs in various firing modes; the change of firing mode is included in the figure. The red line indicates the switch from the lean-lean firing mode to the partially premixed firing mode and the green line indicates the switch from the partially premixed to the premixed steady state firing mode. In the last mode all the burners are fully premixed.

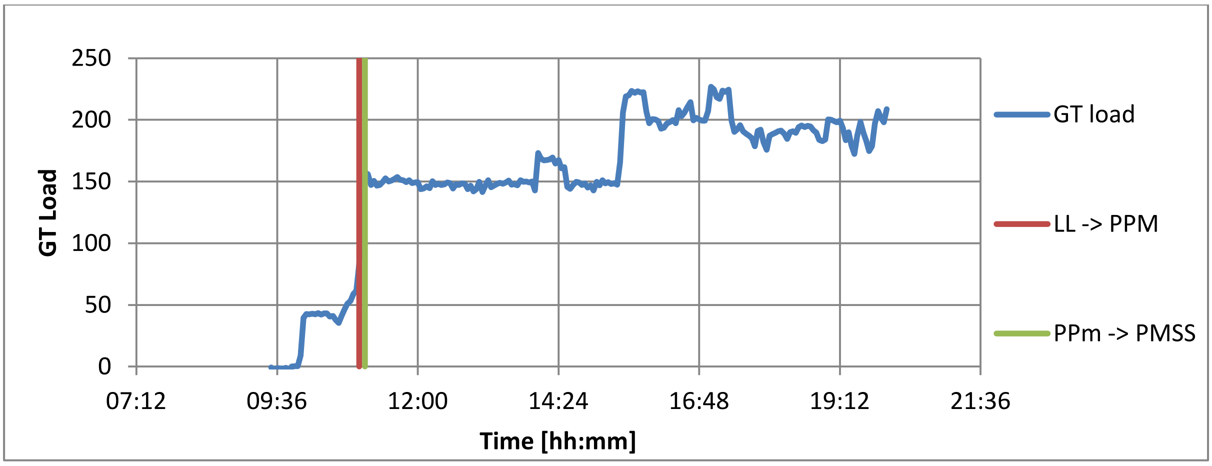

Figure 45 Gas turbine load profile including the various firing modes

Due to the design of the GE 9FA not all the burners operate the same way. The tertiary burner always operates as a fully premixed burner, while the secondary burners have a primary burner attached which uses a diffusion flame allowing combined operation of both burner types.

To minimise combustion dynamics the secondary and tertiary burners do not have the same equivalence ratio. Their equivalence ratios are shown in Figure 46 below. During the lean-lean firing mode the tertiary burner has a significantly higher equivalence ratio than in the premixed steady state mode.

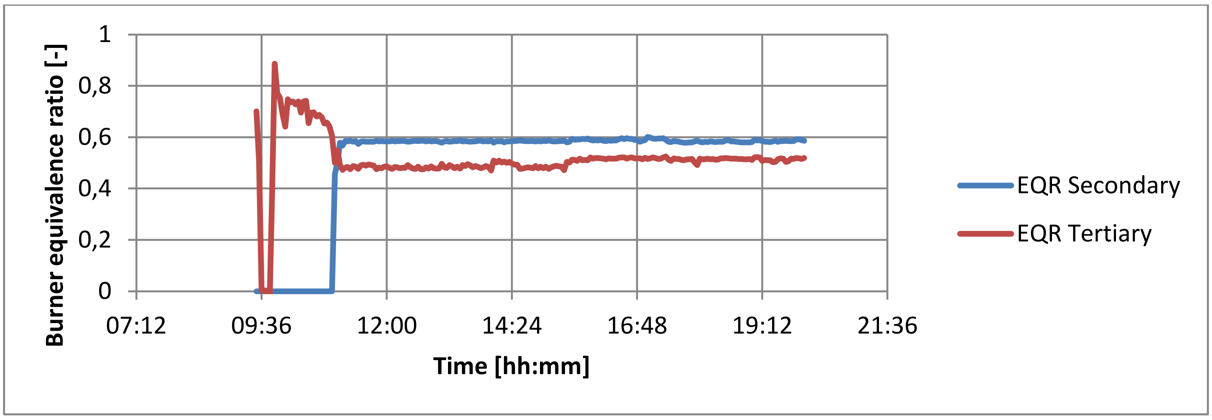

Figure 46 Equivalence ratios of the secondary and tertiary burners

The consequence of the increase in equivalence ratio is the increase in laminar flame speed that it causes, which will lead to an increase in the turbulent flame speed as seen before. To investigate the flashback likelihood the ratio of the laminar and turbulent flame speed with the mean flow velocity is plotted in Figure 47. As these ratios are the largest in the lean-lean firing mode it is the likeliest that flashback will occur there, because the flame speed is the highest here, therefore the focus will be on this region.

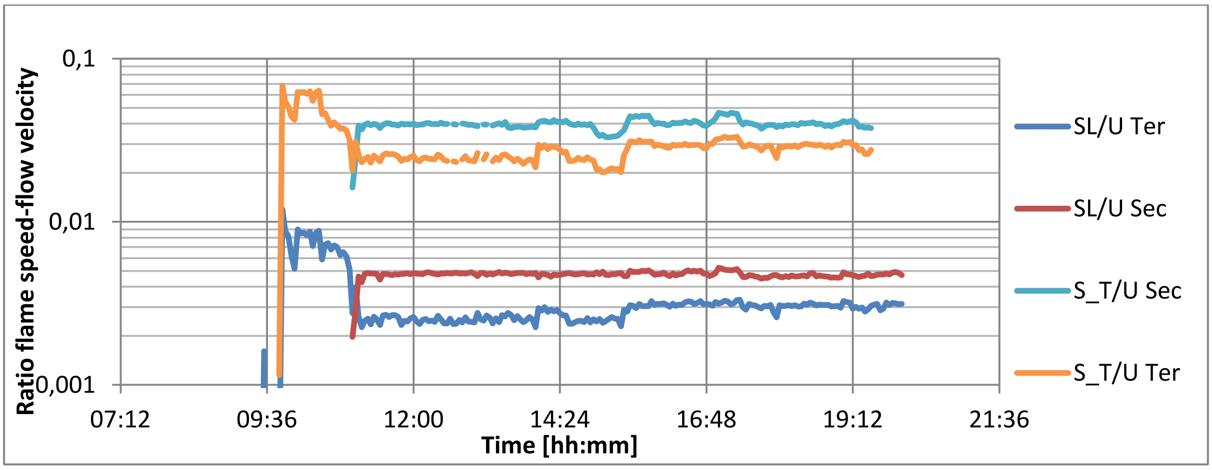

Figure 47 Flame speed bulk flow velocity ratios of both burners

To get an idea of the change in flashback risk a comparison is made between a typical operating point in the lean-lean firing mode and premixed steady state firing mode. The operating points are taken from the tertiary burner. The parameters at these typical operating points and their change when hydrogen is added are shown in Table 14. In the calculations in the table methane replaced natural gas as fuel.

	EQR (ϕ)	Pressure [bar]	Temperature [K]	U_{air} [m/s]	S_L [m/s]	S_T [m/s]	S_L/U [-]	S_T/U [-]
LL 0%H2	0.7	8	585	45.4	0.336	1.78	0.007	0.039
LL 10%H2	0.694	8	585	45.4	0.337	2.06	0.007	0.045
LL 20%H2	0.688	8	585	45.4	0.34	2.22	0.007	0.049
PMSS 0%H2	0.51	13	636	42.8	0.127	0.92	0.003	0.020
PMSS 10%H2	0.505	13	636	42.8	0.128	1.08	0.003	0.024
PMSS 20%H2	0.501	13	636	42.8	0.129	1.17	0.003	0.026

Table 14 Comparing two typical operating points in the load range of the gas turbine and the effects of hydrogen

The table above indicates that hydrogen will increase the likelihood of flashback as the flame speed increases. In the lean-lean mode the ratio of the flame speed and velocity is the largest making this firing mode the most prone to flashback. This indicates that the effects of hydrogen on the flashback likelihood will be the greatest during the start up of the gas turbine and not at conditions comparable to base load.